Coordinated carbenes from electron-rich olefins on $RuHCl(PPr^i_3)_2$†

Joseph N. Coalter III,[a] John C. Bollinger,[a] John C. Huffman,[a] Ulrike Werner–Zwanziger,[a] Kenneth G. Caulton,*[a] Ernest R. Davidson,*[a] Hélène Gérard,[b] Eric Clot[b] and Odile Eisenstein*[b]

[a] *Department of Chemistry and Molecular Structure Center, Indiana University, Bloomington, IN 47405-4001, USA. E-mail: caulton@indiana.edu; davidson@indiana.edu*

[b] *Laboratoire de Structure et de Dynamique des Systèmes Moléculaires et Solides (UMR 5636), Université de Montpellier 2, CC 14, Place E. Bataillon, 34095 Montpellier cedex 5, France. E-mail: odile.eisenstein@lsd.univ-montp2.fr*

Received* (*in New Haven, CT*) *16th September 1999

Dehydrohalogenation of $RuH_2Cl_2L_2$ (L = PPr^i_3) gives $(RuHClL_2)_2$, shown to be a halide-bridged dimer by X-ray crystallography; the fluoride analog is also a dimer. $(RuHClL_2)_2$ reacts with N_2, pyridine and C_2H_4 (L′) to give $RuHClL'L_2$, but with vinyl ether and vinyl amides, H_2C=CH(E) [E = OR, NRC(O)R′] such olefin binding is followed by isomerization to the heteroatom-substituted carbene complex L_2HClRu=$C(CH_3)$(E). The reaction mechanism for such rearrangement is established by DFT(B3PW91) computations, for C_2H_4 as olefin (where it is found to be endothermic), and the structures of intermediates are calculated for H_2C=C(H)(OCH_3) and for cyclic and acyclic amide-substituted olefins. It is found, both experimentally and computationally, that the amide oxygen is bonded to Ru, with a calculated bond energy of approximately 9 kcal mol^{-1} for an acyclic model. Less electron-rich vinyl amides or amines form η^2-olefin complexes, but do not isomerize to carbene complexes. Calculated ΔE values for selected "competition" reactions reveal that donation by both Ru and the heteroatom-substituted X are necessary to make the carbene complex L_2HClRu=$C(X)(CH_3)$ more stable than the olefin complex $L_2HClRu(\eta^2$-H_2C=CHX). This originates in part from a diminished endothermicity of the olefin → carbene transformation when the sp^2 carbon bears a π-donor substituent. The importance of a hydride on Ru in furnishing a mechanism for this isomerization is discussed. The compositional characteristics of Schrock and Fischer carbenes are detailed, it is suggested that reactivity will *not* be uniquely determined by these characteristics, and these new carbenes $RuHCl[C(X)CH_3]L_2$ are contrasted to Schrock and Fischer carbenes.

We reported recently[1] that 16-electron $Ru(H)_2Cl_2L_2$ (L = PPr^i_3) can be dehydrohalogenated to give 14-electron $RuHClL_2$, which has an unusual structure of a *cis*-divacant octahedron [eqn. (1), but *vide infra*].

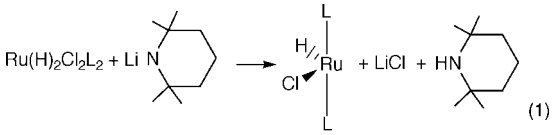

(1)

A

We have come to see that one special advantage of this geometry is that it has two empty sites *cis* and *trans* to H. Coordination of the substrate occurs preferably *trans* to Cl (smaller *trans* influence) and thus *cis* to H. This can facilitate the interaction between RuH and substrate. In contrast, the strong *trans* effect of hydride puts the empty orbital of five-coordinate d^6 16-electron species of the $MHX(CO)L_2$, *etc.*, type *trans* to the hydride [eqn. (2)]

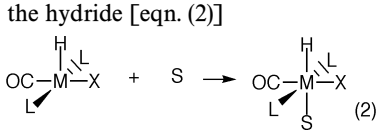

(2)

and the resulting adduct is thus less suitable for rapid reaction between H and substrate S. This has major impact on the kinetics of substrate transformation.[2]

We report here a wide-ranging study of the surprising ways in which $RuHClL_2$ rearranges olefins bearing π-donor substituents on a vinylic carbon, as well as those carrying donor functionality at more remote sites. This furnishes an unusually simple preparation of a class of carbene ligands that does not rely on the conventional routes to carbenes: alkali metal alkyls and α-H abstraction [*e.g.*, eqn. (3)], diazoalkanes [eqn. (4)], and addition of nucleophile, then electrophile to metal carbonyls [eqn. (5)]. This new method relies on the spontaneous (*i.e.*, exothermic) rearrangement of free, then coordinated vinyl ethers to carbene complexes by a ruthenium monohydride [eqn. (6)]. In this paper, we investigate experimentally the scope of this reaction, as well as the origin of this thermodynamic preference using DFT calculations. The calculations will lead to a further clarification of these results in terms of the two "classes" of carbene ligands, the "Schrock type" as formed in eqns. (3) and (4), and the "Fischer type", as produced in eqn. (5).

$$MCl_2 + 2\ RCH_2Li \rightarrow M(CH_2R)_2 \rightarrow M(CHR) + RCH_3 \quad (3)$$

$$M + N_2CHR \rightarrow M(CHR) + N_2 \quad (4)$$

$$M(CO) + Nu \longrightarrow M(CO)Nu \xrightarrow{E^+} [M{=}C(OE)(Nu)]^+ \quad (5)$$

$$H_2C{=}C(OR)H \xrightarrow{RuH} HRu{=}C(OR)(CH_3) \quad (6)$$

Results

$(RuHClL_2)_2$

This molecule is synthesized over a 12 h period in pentane [eqn. (1)]. The molecule shows diastereotopic Pr^i methyl

† Non-SI units employed: 1 torr ≈ 133 Pa; 1 kcal ≈ 4.18 kJ.

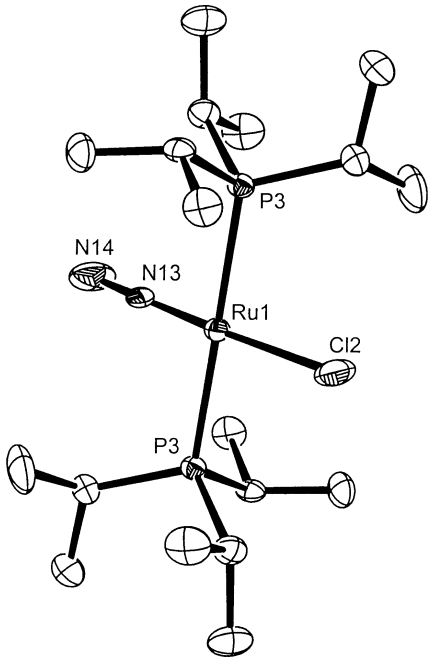

Fig. 1 ORTEP drawing of the nonhydrogen atoms of $RuHCl(N_2)(PPr^i_3)_2$ showing selected atom labeling. The hydride was not located.

hydrogens, which not only rules out a planar structure, but was interpreted earlier as indicating a "saw horse" monomeric structure **A**. Both the ^1H and the $^{31}P\{^1H\}$ NMR spectra show only broadening, but no clear decoalescence at −95 °C in toluene-d_8. Crystals grown for an X-ray diffraction structure determination reveal the molecule to be the dimeric $[RuH(\mu\text{-}Cl)L_2]_2$.[3] The fluoride analog has also been shown to be a dimer by both multi-nuclear NMR and X-ray crystallography. However, since $RuHClL_2$ forms an adduct (see Fig. 1 and Tables 1 and 2) with a reagent as weak as N_2 (1 atm, 25 °C, time of mixing), the inhibiting influence of the chloride bridges is insignificant, and the reagent will be written here as the monomer for simplicity.

$RuHClL_2$ and equimolar pyridine form a 1 : 1 adduct in benzene within the time of mixing. The hydride chemical shift, −20.9 ppm, is sufficiently upfield to suggest that there is no ligand *trans* to hydride, and the coordinated pyridine shows five proton and five ^{13}C chemical shifts, consistent with no facile rotation about the Ru ← N bond. This is a symptom of a crowded environment, and addition of two equivalents of pyridine reveals formation of two new species, in addition to $RuHClL_2(py)$, which are assigned as bispyridine adduct $RuHClL_2(py)_2$ (**a**) and five-coordinate $RuHClL(py)_2$ (**b**). The downfield hydride chemical shift of **a** (−12.9 ppm, t, $^2J_{P\text{-}H}$ = 14 Hz) and the upfield signal with loss of coupling to one phosphine (free phosphine is also observed) for **b** (−20.0 ppm, d, $^2J_{P\text{-}H}$ = 30 Hz) support these assignments and help illustrate this crowding.

The methyl protons of $RuHCl(PPr^i_3)_2$ exchange over a period of several hours with the deuterons of C_6D_6. Presumably this takes place by generation of $RuDCl(PPr^i_3)_2$ and C_6D_5H, followed by the ruthenium deuteride scrambling into the phosphines as discussed below. The phenomenon is detected by ^1H NMR *via* a large increase in the protio signal of benzene-d_6, coupled with a decrease and broadening of the signals for Ru–H and the Pr^i methyl groups when $RuHCl(PPr^i_3)_2$ is placed in a flame-sealed NMR tube and periodically monitored for 2 days.

Reactivity of $RuHClL_2$ towards hydrocarbon olefins

$RuHClL_2$ binds ethylene (1 atm or equimolar, 20 °C) to give a 1 : 1 adduct. The hydride chemical shift, −22.0 ppm, is still sufficiently upfield to suggest that there is no ligand *trans* to hydride, consistent with structure **B**.

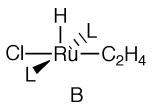

B

Table 1 Crystallographic data

	$RuHCl(PPr^i_3)_2(C_6H_9NO)$	$RuHCl(N_2)(PPr^i_3)_2$
Formula	$C_{24}H_{52}ClNOP_2Ru$	$C_{18}H_{43}ClN_2P_2Ru$
Formula weight	569.15	486.02
Crystal system	monoclinic	monoclinic
Space group	$P2_1/a$	$P2_1/c$
a/Å	16.124(5)	7.9985(10)
b/Å	11.289(4)	8.9047(11)
c/Å	16.313(5)	16.614(2)
β/°	100.30(1)	92.180(10)
U/Å^3	2921.59	1182.5(2)
Z	4	2
T/°C	−171	−171
$\mu(MoK_a)$/cm^{-1}	7.5	9.0
Meas. reflections	5136	6389
Indep. reflections	4692	6212
R_{int}	0.027	0.030
R^a	0.0460	0.0346
R_w [a]	0.0349	0.0675

[a] $R = \Sigma \| F_o | - | F_c \| / \Sigma | F_o |$; $R_w = [\Sigma w(| F_o | - | F_c |)^2 / \Sigma w | F_o |^2]^{1/2}$ where $w = 1/\sigma^2(| F_o |)$.

Table 2 Selected bond distances (Å) and angles (°) for $RuHCl(N_2)(PPr^i_3)_2$

Ru(1)–Cl(2)	2.396(4)	Ru(1)–N(13)	1.84(2)
Ru(1)–P(3)	2.3727(10)	N(13)–N(14)	1.10(2)
Cl(2)–Ru(1)–P(3)	89.29(13)	P(3)#1[a]–Ru(1)–N(13)	89.2(5)
Cl(2)–Ru(1)–P(3)#1	90.71(13)	Ru(1)–N(13)–N(14)	175(2)
P(3)–Ru(1)–N(13)	90.8(5)		

[a] P(3)#1 is related to P(3) by the inversion center.

Although this is the ground state structure of this molecule, reaction of $RuHClL_2$ with excess C_2D_4 in C_6H_6 for 1 h at 20 °C shows (^2H NMR) deuteration of the H on Ru and also the methyl groups of coordinated PPr^i_3. This is indicative of reversible insertion of C_2D_4 into the Ru–H bond and it also indicates that the 16-electron olefin hydride form (**B**) is more stable than $Ru(C_2H_5)ClL_2$. Deuteration of the Pr^i methyls is accounted for by reversion to $RuDCl[P(CH(CH_3)_2)_3]_2$ and then CH_3/RuD scrambling, as was independently established for this species deuterated by two independent methods. Insertion of ethylene into Ru–H is also evidenced by the formation of ethane, detected by ^1H NMR. Its formation most likely occurs by alkane elimination from unstable $Ru(C_2H_5)ClL_2$, which has oxidatively added an Pr^i methyl group (C–H). This C–H activation also offers an additional explanation for deuteration of the Pr^i methyl with C_2D_4. The metal-containing products after CH_3CH_3 elimination could not be identified. There is no isomerization of ethylene into the carbene ligand $CH(CH_3)$.

$RuHClL_2$ also reacts within 30 min with the olefins 1-hexene and styrene, but only 10% adduct is formed, with unreacted $RuHClL_2$ comprising the bulk of the resulting mixture at 25 °C. Both these adducts are identified by a new hydride signal in ^1H NMR (−23.7 ppm, m, for 1-hexene and −22.1 ppm, apparent triplet, for styrene) and corresponding $^{31}P\{^1H\}$ NMR AB patterns centered at 37.2 ppm ($^2J_{P\text{-}P} = 287$ Hz) for 1-hexene and at 85.9 ppm ($^2J_{P\text{-}P} = 34$ Hz) for styrene. The spectroscopic similarity of the ethylene, 1-hexene, and ethyl vinyl ether adducts and large difference of the styrene adduct suggests that styrene may coordinate differently (perhaps as $\eta^2 : \eta^{1-2}$-vinyl : arene or η^{2-4}-arene). Longer reaction times yield no carbenes, but only complex mixtures of products.

Reactivity of $RuHClL_2$ towards vinyl ethers

$RuHClL_2$ rapidly effects a formal 1,2-hydrogen migration [eqn. (7)] of vinyl ethers into the coordinated carbene. The reaction occurs for a variety of groups R, including those with $SiMe_3$, ether, alcohol, tertiary amino, fluoro, and epoxide functionality. All products show diastereotopic Pr^i methyl groups, consistent with the presence of three different substituents, H, Cl and carbene, on Ru. While this reveals nothing about the square pyramidal *vs.* trigonal bipyramidal geometry around Ru, the hydride chemical shifts (Table 3), rather far upfield (−21 ppm), could be interpreted in terms of the hydride being approximately *trans* to an empty site (*i.e.*, square pyramidal). The hydride chemical shift is thus also perhaps the most generally sensitive indicator of whether there is a ligand (from functionality in the substituent R) coordinated *trans* to hydride. The similarity of the hydride chemical shift for R = Et (Table 3) to those for all components with functionalized alkyl groups in eqn. (7) suggests that none of the latter O, N or F donors coordinates to Ru.[4] Perhaps this is caused by the difficulty of forming six-membered rings. For the case of F, this conclusion is reinforced by a ^{19}F chemical shift that lies within 1 ppm of that of the free olefin, and by the absence of coupling to F in the ^{31}P NMR spectrum. Even at −80 °C, ^{19}F NMR spectra reveal that F remains uncoordinated.

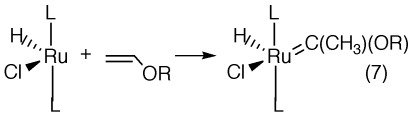

(7)

R = Et, Cy, $SiMe_3$, $CH_2CH_2OBu^n$, CH_2CH_2OH, $(CH_2CH_2O)_2H$, CH_2CH_2F, $CH_2CH_2NEt_2$, CH_2CHOCH_2

When O is from an epoxide ring, the presence of a chiral carbon β to the vinyloxy oxygen necessitates phosphine inequivalence. From the magnitude of their $^{31}P\{^1H\}$ NMR (Fig. 2) chemical shift difference [$\Delta\delta = only$ 0.09 ppm (15 Hz), $^2J_{P\text{-}P} = 220$ Hz], it is safe to assume that the chiral center is far from the phosphorus atoms, indicating no epoxide binding to ruthenium.

The case of dihydrofuran [eqn. (8)] is interesting as it shows that a cyclic internal vinyl ether is also easily isomerized.[5] The hydride chemical shift is consistent with no donation to Ru by

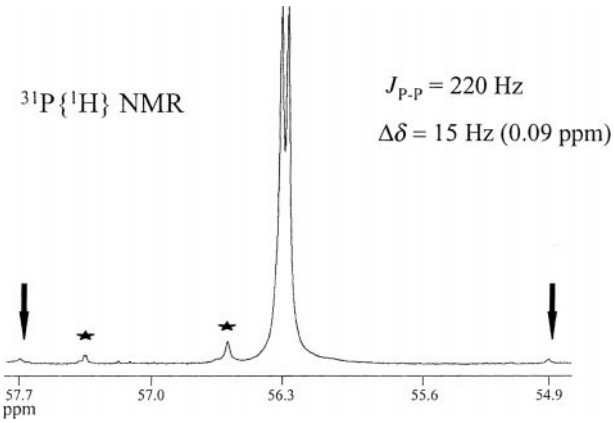

Fig. 2 $^{31}P\{^1H\}$ NMR (162 MHz) spectrum of $RuHCl[C(Me)(OCH_2CHOCH_2)](PPr^i_3)_2$, showing the inequivalence of the phosphorus nuclei caused by the epoxide carbon asymmetry. Starred peaks are impurities and the arrows indicate the outer lines of the AB pattern.

Table 3 Selected NMR data as a function of carbene substituent in C_6D_6

	δ Ru–*H*	$^2J_{P\text{-}H}$/Hz	δ Ru=*C*	$^2J_{P\text{-}C}$/Hz	δ Ru–*P*
Vinyl ethers					
OEt	−21.7	23	290	9.7	58.2
$OCH_2CH_2CH_2$–[a,d]	−18.2	22	287	9.4	60.1
OCy	−19.4	23	[b]	[b]	57.4
$OSiMe_3$	−18.0	22	284	8.4	58.6
$OCH_2CH_2OBu^n$	−21.3	22	289	9.5	57.8
CH_2CH_2OH	−21.1	22	289	8.4	56.4
$(OCH_2CH_2)_2OH$	−21.4	21	[b]	[b]	56.3
–OCH_2CH_2O–[e]	−21.2	22	289	9.1	57.9
OCH_2CH_2F	−21.3	22	[b]	[b]	57.8
$OCH_2CH_2NEt_2$	−21.4	[c]	[b]	[b]	56.4
OCH_2CHOCH_2	−21.4	22	[b]	[b]	57.7
Vinyl amides					
N(Me)C(O)Me[f]	−17.2	26	265	9.7	50.4
$NC(O)CH_2CH_2CH_2$–[d,f]	−19.6	26	262	10	49.3

[a] ^1H data reported in CD_2Cl_2. [b] Not measured. [c] Not resolved (broad). [d] Cyclic. [e] Dimetal carbene. [f] All NMR data in CD_2Cl_2.

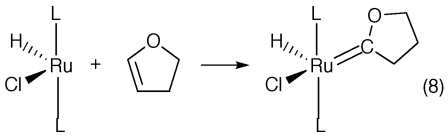

(8)

the ether β-oxygen, just as it does not occur for the products in eqn. (7). Using the symmetrical difunctional vinyl ether as in eqn. (9), with slow addition of the vinyl ether to $RuHClL_2$, a dimetal carbene is produced.

$$RuHClL_2 + 1/2\ CH_2{=}CH(OCH_2CH_2O)CH{=}CH_2 \rightarrow$$
$$L_2ClHRu{=}C(Me)(OCH_2CH_2O)(Me)C{=}RuHClL_2 \quad (9)$$

The presence of inequivalent (*i.e.*, H and Cl) substituents on Ru, together with the carbene plane *not* eclipsing the RuP_2 plane,[6] makes two isomers (**C** and **D**) possible for an unsymmetrically substituted carbene, CRR′. Indeed, upon lowering

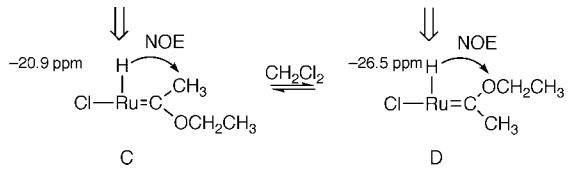

C D

the temperature in toluene-d_8, one observes broadening, then decoalescence and sharpening of the Ru–H, the C–CH_3 and the OCH_2 ^1H NMR signals of two isomers (**C** and **D**) with a population ratio of more than 10 : 1. The $^{31}P\{^1H\}$ NMR confirms this, with decoalescence at about −50 °C and two separate resonances (major isomer at 55.8 and minor at 51.2 ppm) resolved below −70 °C. Lineshape analysis of the $^{31}P\{^1H\}$ NMR spectrum gives $\Delta G‡ = 9.8$ kcal mol^{-1} for **C** → **D** at −60 °C. The assignment of isomer structure to spectra was done by NOE experiments of the hydrides at −95 °C. The large (5 ppm) difference in the hydride chemical shift of these isomers supports their being isomeric around the Ru=C bond and not around the C(carbene)–OEt bond. These observations are significant because (1) no previously known compound has had suitable symmetry to prove that carbene rotation is rapid at 25 °C and (2) carbene rotation is an essential step in the olefin metathesis[6] process (*i.e.*, forming the metallacyclobutane).

Mechanism. The reaction of equimolar $RuHClL_2$ with ethyl vinyl ether is immediate and complete at −65 °C in toluene-d_8 to give a primary product whose ^{31}P and ^1H NMR are consistent with a 1 : 1 olefin adduct. The $^{31}P\{^1H\}$ NMR (Fig. 3) is an AB pattern ($J_{P\text{-}P_B} = 300$ Hz), indicating that the unsymmetrical olefin substituents are bound such that the phosphines are inequivalent (but transoid).[7]

Carbene product formation demands cleavage of the C–D bond in $H_2C{=}C(D)(OEt)$, but at least three mechanisms (Scheme 1) can be envisioned: (*a*) direct C–D oxidative addition to the ruthenium hydride, followed by hydrogen migration to the vinyl C_β, (*b*) primary addition of Ru–H to C=C, followed by α-hydrogen migration to Ru, (*c*) concerted 1,2-hydrogen migration within the coordinated olefin. These have distinct predictable consequences for the deuterium label since (*a*) mixes RuH with C–D, (*b*) migrates D exclusively to Ru only after the Ru–H has been cleaved, and (*c*) migrates D exclusively to the CH_2 carbon. In fact, when $RuHClL_2$ and $H_2C{=}CD(OEt)$ are combined at −40 °C and observed by ^2H NMR beginning at −20 °C, one sees immediately $RuDCl(olefin)L_2$ in which there is also D in the phosphine methyl groups, and some free $HDC{=}CH(OEt)$. These indicate reversible olefin binding to Ru and reversible migration of H (or D) from Ru to *both* olefinic carbons [eqn. 10)].

The scrambling of D into the phosphine methyls was already established as a characteristic of $RuDClL_2$ itself. It is thus

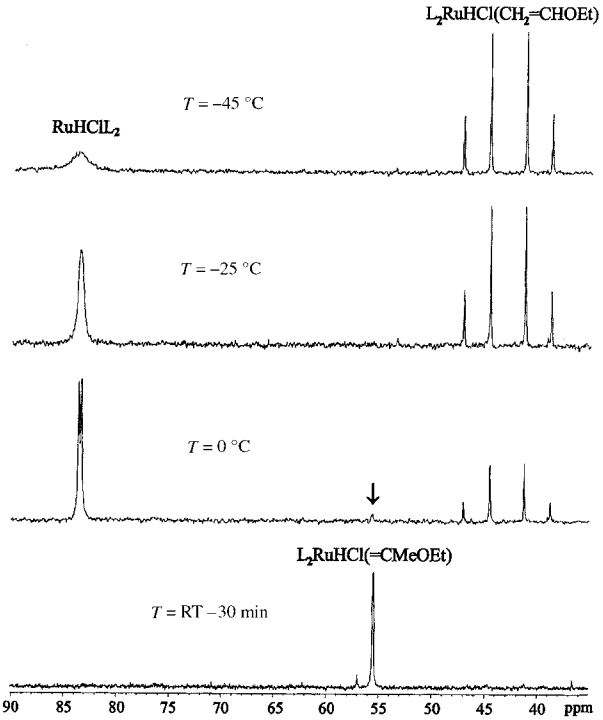

Fig. 3 $^{31}P\{^1H\}$ NMR monitoring of reaction progress when $RuHClL_2$ and $H_2C{=}CH(OEt)$ are combined at −65 °C in toluene-d_8. Doublet in $RuHClL_2$ signal is due to incomplete hydride decoupling. Arrow shows initial growth of carbene product at 0 °C.

clear that Ru–H adds in both directions to the olefin, but only one of these leads to carbene product; the regiochemistry of carbene production is *not* caused by selectivity in the initial H migration step. By 0 °C, carbene product grows in, with D both at Ru (25%) and at the carbene methyl (75%). Thus, attempts to establish mechanism by quantitative comparison to the predictions of eqn. (10) are frustrated by general isotope scrambling.[8] However, the significantly *slower* reaction rate observed using $H_2C{=}CD(OEt)$ establishes that C–D cleavage occurs before or at the rate determining step. From the scrambling patterns observed, we propose that the most likely mechanism of carbene formation combines mechanism b of Scheme 1 and eqn. (10).

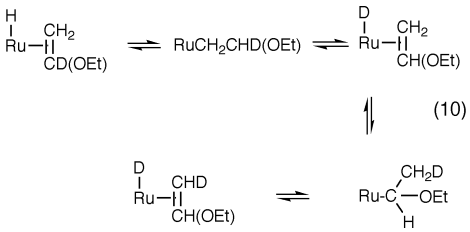

(10)

Reactivity of $RuHClL_2$ towards vinyl amides

The vinyl amides are also transformed into the carbenes shown in eqn. (11). The chemical shifts of the carbene carbon, of the hydride, and of ^{31}P are all sufficiently different from those in eqn. (7) to suggest the possibility of amide oxygen coordination. Interestingly, there is a large difference in the ^1H NMR chemical shift of Ru–H and in the ν(CO) of the pendant

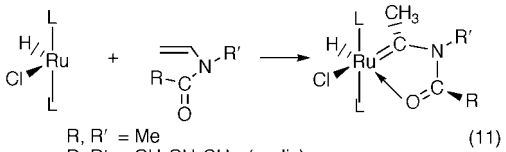

R, R′ = Me
R, R′ = $CH_2CH_2CH_2$ (cyclic) (11)

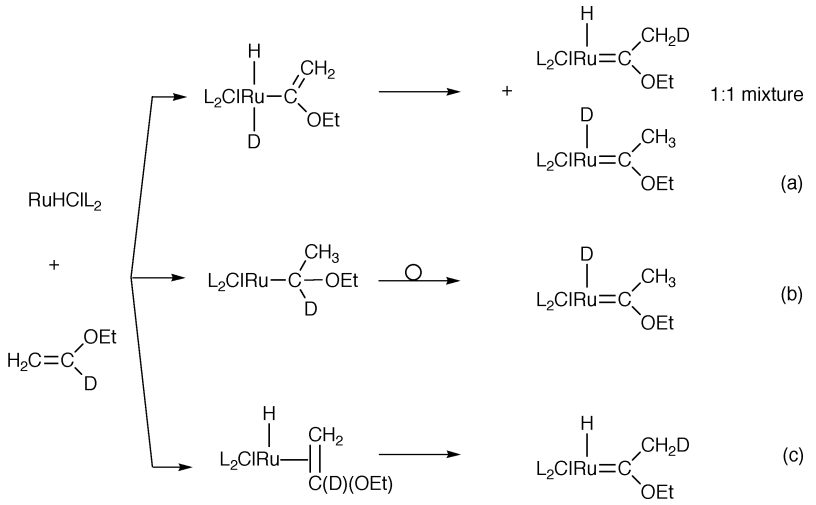

Scheme 1

amide between the products from cyclic and acyclic vinyl amides (R,R′ = Me: $\delta = -17.2$ $\nu(CO) = 1599$ cm^{-1}; R,R′ = $CH_2CH_2CH_2$: $\delta = -19.6$ $\nu(CO) = 1640$ cm^{-1}). These data show that while both compounds may have C=O metal-bound, the geometric constraints at the cyclic species hinder its binding relative to the carbene derived from acyclic *N*-methyl-*N*-vinyl acetamide. Carbonyl oxygen coordination was confirmed by an X-ray crystal structure determination for the product from 2-vinyl pyrrolidinone (Table 4 and Fig. 4). The structure is derived from the five-coordinate carbene complexes Ru(carbene)Cl(H)L_2 by addition of the pendant carbonyl functionality of the carbene in the site *trans* to hydride. The inner coordination sphere has idealized mirror symmetry, which extends even to the conformations of all Pr^i groups. Bond angles in the six-coordinate polyhedron are generally within 10° of the ideal 90°, except for within the five-membered ring of the bidentate carbene/amide ligand [79.45(17)°]; also the phosphorus nuclei deviate visibly from octahedral symmetry [∠ P–Ru–P = 158.67(5)°] and they bend main ly towards hydride and sligtly towards chloride. The Ru–C(carbene) distance is short (but not as short as to a carbonyl ligand[9]) and the distance to Cl *trans* to carbene is unusually long [2.5387(14)Å]. The Ru ← O distance is not especially long, in spite of its being *trans* to hydride. There is no trace of interaction between the mutually *cis* ligands hydride and carbene; hydride lies in the nodal plane of the Ru=C bond. The distance from N28 to the carbene carbon is 8σ (0.063 Å) longer than to the carbonyl carbon (C24), which suggests that the N–C π bond is more in the amide group, and less to the carbene carbon [eqn (12)].

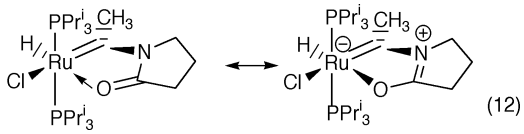

(12)

The amide reactions proceed considerably slower than those with vinyl ethers, taking 2–4 days to react completely. After 1 h in C_6D_6, the mixture of 2-vinyl pyrrolidinone and $RuHClL_2$ exhibits ^1H and ^{31}P NMR signals for three major intermediates, as well as for starting material and final product. One intermediate exhibits an AX pattern (δ 57.6, 33.4; $^2J_{P\text{-}P} = 274$ Hz) in the ^{31}P spectrum and an *apparent* triplet in ^1H NMR (δ −29.2, $^2J_{P\text{-}H} = 34.8$ Hz) while the other two show singlets in ^{31}P (δ 85.6, 74.7) and Ru–H *doublets* in ^1H (δ −10.1, −19.6; $^2J_{P\text{-}H} = 33.0$, 35.1 Hz, respectively). These latter intermediates are consistent with dissociation of phosphine and indeed free phosphine is observed by ^{31}P NMR. Upon completion of the reaction, phosphine re-coordination occurs, with the only product seen being the amido-substituted carbene. Although the exact nature of all intermediates cannot be inferred (coordination by olefin, N, η^2-carbonyl, or a combination of these groups all produce inequivalent phosphines), the multiple coordination modes of vinyl amides, coupled with the possibility of required phosphine dissociation, help explain the kinetic sluggishness of this reaction.

Reaction of equimolar $RuHClL_2$ and *N*-vinyl phthalimide leads to **E**, which does not rearrange to a carbene isomer over 20 h at 25 °C. After this time, substantial decomposition of product occurs in solution. Complex **E** shows inequivalent

Table 4 Selected bond distances (Å) and angles (°) for $RuHCl(PPr^i_3)_2(C_6H_9NO)$

Ru(1)–Cl(2)	2.5387(14)	O(23)–C(24)	1.245(6)
Ru(1)–P(3)	2.3658(15)	N(28)–C(24)	1.350(6)
Ru(1)–P(13)	2.3664(15)	N(28)–C(27)	1.476(6)
Ru(1)–O(23)	2.273(3)	N(28)–C(29)	1.413(6)
Ru(1)–C(29)	1.880(5)	Ru(1)–H(1)	1.25(4)
P(3)–Ru(1)–P(13)	158.67(5)	C(24)–N(28)–C(29)	118.0(4)
P(3)–Ru(1)–O(23)	99.96(10)	C(27)–N(28)–C(29)	129.8(4)
P(3)–Ru(1)–C(29)	92.84(14)	Ru(1)–C(29)–N(28)	114.7(3)
P(13)–Ru(1)–O(23)	100.57(10)	Ru(1)–C(29)–C(30)	133.8(4)
P(13)–Ru(1)–C(29)	96.51(14)	N(28)–C(29)–C(30)	111.5(4)
O(23)–Ru(1)–C(29)	79.45(17)	Cl(2)–Ru(1)–H(1)	96.4(16)
Ru(1)–P(3)–C(4)	116.40(19)	P(3)–Ru(1)–H(1)	78.3(16)
Ru(1)–P(3)–C(7)	114.40(7)	P(13)–Ru(1)–H(1)	82.1(16)
Ru(1)–P(3)–C(10)	112.53(18)	O(23)–Ru(1)–H(1)	171.9(16)
Ru(1)–P(13)–C(14)	113.92(18)	C(29)–Ru(1)–H(1)	92.7(16)
Ru(1)–P(13)–C(17)	115.80(19)	Cl(2)–Ru(1)–P(3)	88.06(4)
Ru(1)–P(13)–C(20)	113.68(20)	Cl(2)–Ru(1)–P(13)	85.71(5)
Ru(1)–O(23)–C(24)	106.2(3)	Cl(2)–Ru(1)–O(23)	91.47(9)
C(24)–N(28)–C(27)	112.2(4)	Cl(2)–Ru(1)–C(29)	170.90(15)

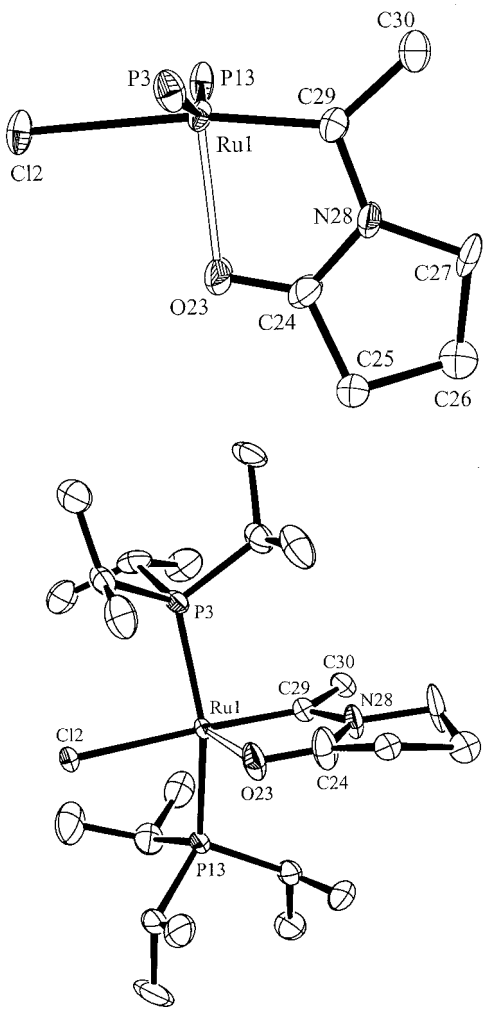

Fig. 4 ORTEP drawing of the nonhydrogen atoms of RuHCl-[C(Me)NC(O)$CH_2CH_2CH_2$](PPr^i_3)$_2$, showing selected atom labeling.

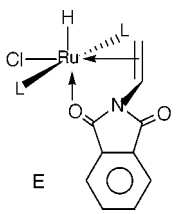

E

phosphines, with ^{31}P chemical shifts of 35.4 and 57.9 ppm and a $J_{P\text{-}P}$, of 278 Hz. These values are very close to those of the *bis* phosphine intermediate detected in reaction with 2-vinyl pyrrolidinone. The large difference in chemical shift of the carbonyl groups by $^{13}C\{^1H\}$ NMR (10 ppm), coupled with a hydride chemical shift similar to the carbenes from vinyl amides, lends evidence for oxygen coordination. Thus, while one keto group on N permits isomerization to a carbene complex, two keto groups apparently leave the nitrogen too weak a donor to stabilize a carbene.

It is of interest that 9-vinylcarbazole (**F**) is not too bulky to bind to $RuHClL_2$, but the reaction does not proceed to a carbene complex, perhaps because the nitrogen lone pair is too involved in the arene π system to stabilize the electrophilic carbene **G**, which would also be very crowded. It is clear that

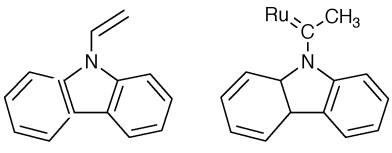

F G

nitrogen is not the donor site in the observed adduct since the phosphines are inequivalent, as they would be in a π-olefin structure.

Reactivity with a conjugated diene ether substrate

Addition of 10 equiv. of the conjugated diene, 3-methylene-2,3-dihydrofuran, to a solution of $RuHCl(PPr^i_3)_2$ in C_6D_6 results in complete isomerization to 3-methylfuran within 10 min. [eqn. (13)].

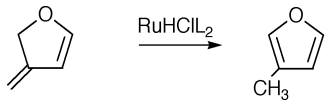

(13)

No reaction occurs from 3-methylfuran with $RuHCl(PPr^i_3)_2$ at room temperature over several hours. This isomerization is consistent with addition of Ru–H across the terminal alkene to give the *tertiary* alkyl, followed by β-H elimination to achieve aromatic stabilization in the resulting furan.

DFT computation of the ethylene → methyl carbene isomerization

The isomerization of free ethylene into free methyl carbene is known to be a very endothermic reaction (80 kcal mol^{-1}). Recent laser flash photolysis experiments and *ab initio* calculations on propene have shown that the energy of reaction is 60 kcal mol^{-1} endothermic.[10] Isomerization of free olefin is thus unlikely to happen in less extreme conditions (*i.e.*, in solution).

The reaction path for transforming ethylene into its isomer $C(H)CH_3$ in the presence of $RuHCl(PH_3)_2$ [**Ru**] (as a model for $RuHClL_2$) was determined with DFT(B3PW91) calculations (Fig. 5). As mentioned earlier, the 14-electron fragment $RuHClL_2$ does not exist as an isolated species. However, it is a reasonable assumption to consider that the olefin causes the dissociation of the dimer into two monomeric $RuHClL_2$, which is stabilized through coordination to the olefin. For the sake of discussion, we will consider that the starting entities are thus [**Ru**] and C_2H_4.

The olefin coordinates [**Ru**] *trans* to Cl to form a 16-electron intermediate **1**, which is a square-based pyramid with hydride at the apical site. This adduct has the classical geometry of numerous five-coordinate d^6 species. The olefin is coordinated opposite to the ligand with the smaller *trans* influence (Cl). This combination of ligands on the metal forces the olefin to be *cis* to the hydride, which is favorable for further reaction between these two ligands. The orientation of the olefin also is a favorable factor since the C=C bond is found to be aligned with Ru–H. This preferred orientation minimizes the steric effect between the phosphine ligands and the olefin and maximizes the stabilizing *cis* interaction between the hydride and the olefin,[11] although it should be noted that the *cis* effect alone does not make the olefin tilt toward H. The olefin adduct has no other remarkable structural aspects. The binding energy of [**Ru**] to C_2H_4 is quite large (39.2 kcal mol^{-1}), which characterizes the high unsaturation of [**Ru**]. The insertion of the olefin into the Ru–H bond is a facile process since the transition state is found to be only 7.6 kcal mol^{-1} above **1**. It produces an ethyl complex, **2**, which is less stable than **1** by 6.2 kcal mol^{-1}. This ethyl complex has a remarkably strong β agostic C–H bond since the C_β–H bond length is equal to 1.221 Å, while Ru–H is significantly short, 1.774 Å. At the same time, the C–C bond length is significantly shorter (1.482 Å) than that of a single C–C bond and the two Ru–C distances do not differ greatly (2.070 Å and 2.293 Å), although the initial difference in bond lengths between Ru–C_α and Ru–C_β has been increased. The transition state **TS1-2** between **1** and **2** has the expected features of an unsaturated ligand inserting into an Ru–H bond: the ethylene is more unsymmetrically bonded (Ru–C_α = 2.107,

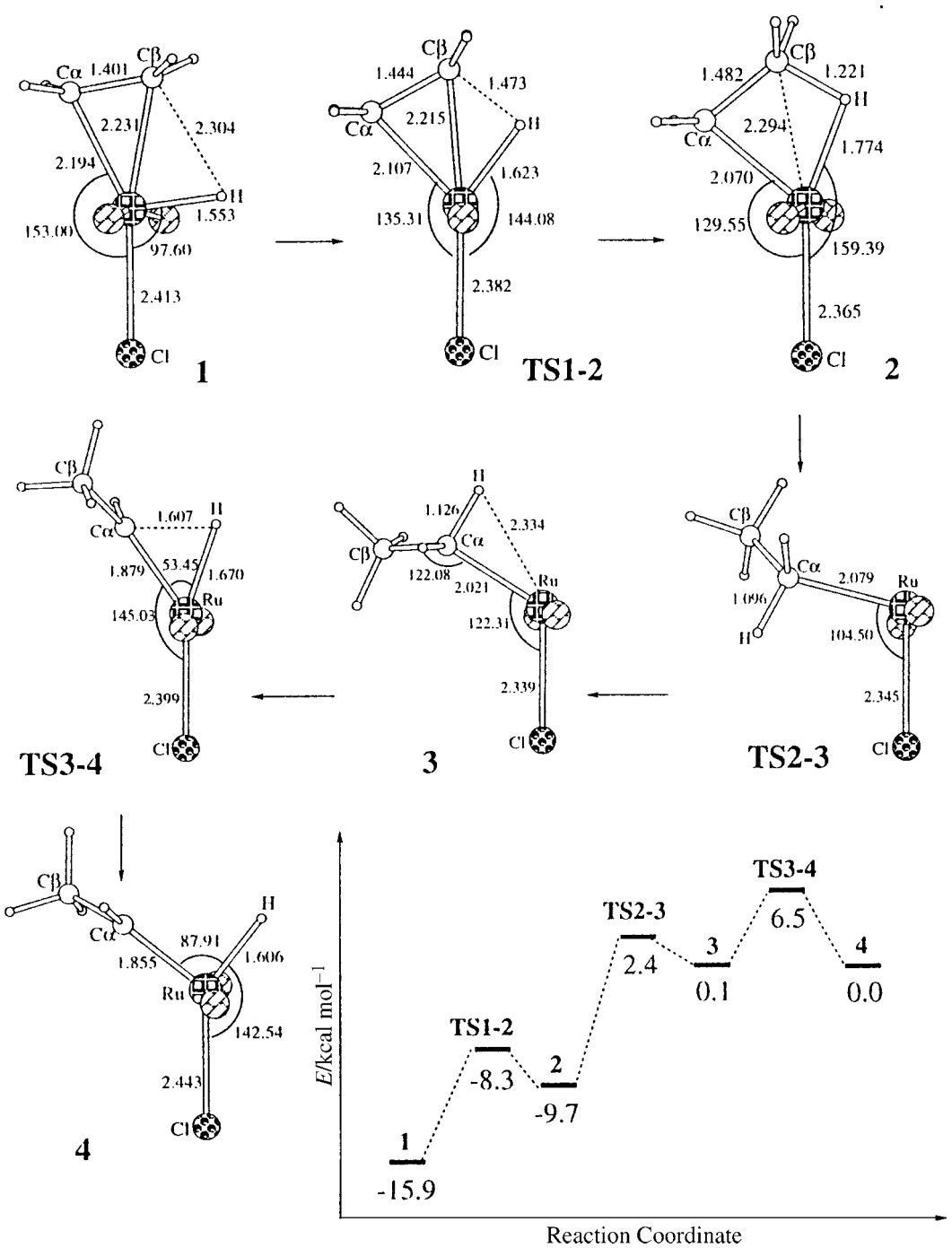

Fig. 5 DFT(B3PW91) optimized structures and energies for $RuC_2H_5Cl(PH_3)_2$ isomers.

Ru–C_β = 2.215 Å) than in **1** and less than in **2**. However, in a nonintuitive manner, C_β has moved closer to Ru than it was in **1**, in an apparent attempt to assist in H–C_β bonding. The C–C bond length (1.444 Å) is intermediate between that in **1** and in **2**. The main change in structure is thus the displacement of H as measured by the Cl–Ru–H angle (97.6°, 144.0°, 159.0° as one goes from reactant to product). According to the Hammond postulate, **TS1-2** should resemble more **2**, to which it is closer in energy, and this is true for the Cl–Ru–H angle and the Ru–$C_{(\alpha}$ distance. However, the behavior of Ru-C_β illustrates some limitation in using the Hammond postulate.

With regard to forming the HRu=C(H)Me moiety, the geometry of **2** is poorly adapted for migrating a hydrogen from C_α to the metal. Rotation of the ethyl group is thus necessary to put an α hydrogen in proximity to the nearest empty orbital of the metal. Rotation of the ethyl is energetically demanding (12.1 kcal mol^{-1}) since it is necessary to break the unusually strong C_β–H agostic bond in addition to rotating about the single Ru–C_α bond. The transition state **TS2-3** has no agostic interaction (closest Ru···H distance = 2.6 Å) and thus the C–C bond length is typical of that of a single bond (1.523 Å). The rotation of the ethyl group leads to **3**, where the ethyl group has an α agostic hydrogen. The energy of this intermediate is 9.8 kcal mol^{-1} above **2**. This is in great part due to the large difference in the strength of the agostic interactions. In **3**, C_α–H (1.13 Å) is much less elongated than C_β–H in **2** and, consequently, the agostic H is much further away from Ru (2.334 Å in **3**). In addition, the C–C bond (1.517 Å) is close to that of a single C–C bond.

Since rotation about the Ru–C_α bond is energetically demanding, we searched for an alternative path. Inversion at the metal center would achieve the requirement to put an α hydrogen in proximity to an empty metal orbital. The transition state, **TS′2-3**, for this transformation was located 33.1

kcal mol^{-1} above **2**. The geometry of this **TS** is square planar. Its high energy shows the strong energetic preference for a bent geometry at a d^6 four-coordinate center.

The α migration from **3**, to the final hydrido carbene complex **4**, is an easy process ($\Delta E\ddagger = 6.4$ kcal mol^{-1}). Remarkably, **3** and **4**, although they are very different in bonding and in formal valence electron count, are isoenergetic. Whatever determines the energies of both of these is responsible for [**Ru**] being unable to isomerize ethylene to ethylidene: the olefin form **1** is more stable and even the β agostic ethyl, **2**, which the calculations suggest to be kinetically accessible at 25 °C, is significantly more stable than **3** and **4**. This accounts for the deuterium scrambling and the absence of an observable quantity of ethylidene complex in the reaction of C_2D_4.

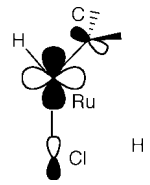

The final product **4** has the geometry of a trigonal bipyramid distorted towards a Y shape through large Cl–Ru–C (129.5°) and Cl–Ru–H (142.5°) angles. The plane of the carbene eclipses the P–Ru–P axes. This conformation permits the empty carbene p orbital to interact with the highest occupied d Ru orbital (**H**). Therefore, bulky phosphines could force a rotation of the carbene plane. It has been shown that the conformation of the carbene in the related $RuCl_2(PR_3)_2(CHR)$ depends on the nature of the substituents at the phosphine and carbene.[6] The transition state **TS3-4** to form **4** has already many geometrical aspects of the final product despite being energetically equidistant from **3** and **4**. The carbene complex is fully formed since the carbon bonded to the metal is planar (sum of the angles at C = 360°). The Ru–C distance is equal to 1.879 Å, very close to that in the final product (1.855 Å). The Ru–H bond is also almost fully formed (1.670 Å) *vs.* 1.606 Å in **4**. The major difference between **TS3-4** and **4** lies in the angles between the three ligands. The Cl–Ru–C angle varies from 145.0° (**TS3-4**) to 129.5° (**4**), while ∠H–Ru–C varies from 53.5 to 87.9°, accordingly. In this last step of the reaction path, as well as in the step of the insertion of ethylene into the Ru–H, there is *no synchronous variation* of all the coordinates from reactants to products (in contrast to the predictions of the Hammond postulate).

DFT computation of the vinyl ether → alkoxy carbene isomerization

The model chosen for CH_2=C(H)OR is CH_2=C(H)OCH_3. The geometry of the vinyl ether coordinated to [**Ru**] has been optimized (Fig. 6). The overall geometry is that of a square pyramid with an apical hydride ligand. The olefin prefers to coordinate the metal in the mirror plane of the molecule, as does ethylene. Even in the absence of large phosphines, the conformation observed experimentally is thus shown to be preferred. Both isomers **5** and **6** (Fig. 6) are found to be minima on the potential energy surface with a preference of 0.9 kcal mol^{-1} for **6**. This almost negligible difference in energy is not due to an O···Ru interaction in **6** since the oxygen is outside of the bonding range to the metal (Ru···O distance>3 Å).

Comparing the ethylene and the CH_2=C(H)OCH_3 adducts, it appears that the substitution by OCH_3 has no significant effect on the geometry of the complex. In **6**, there is a slight decrease in the non-bonding distance between the unsubstituted carbon of CH_2=C(H)OMe and Ru with respect to the

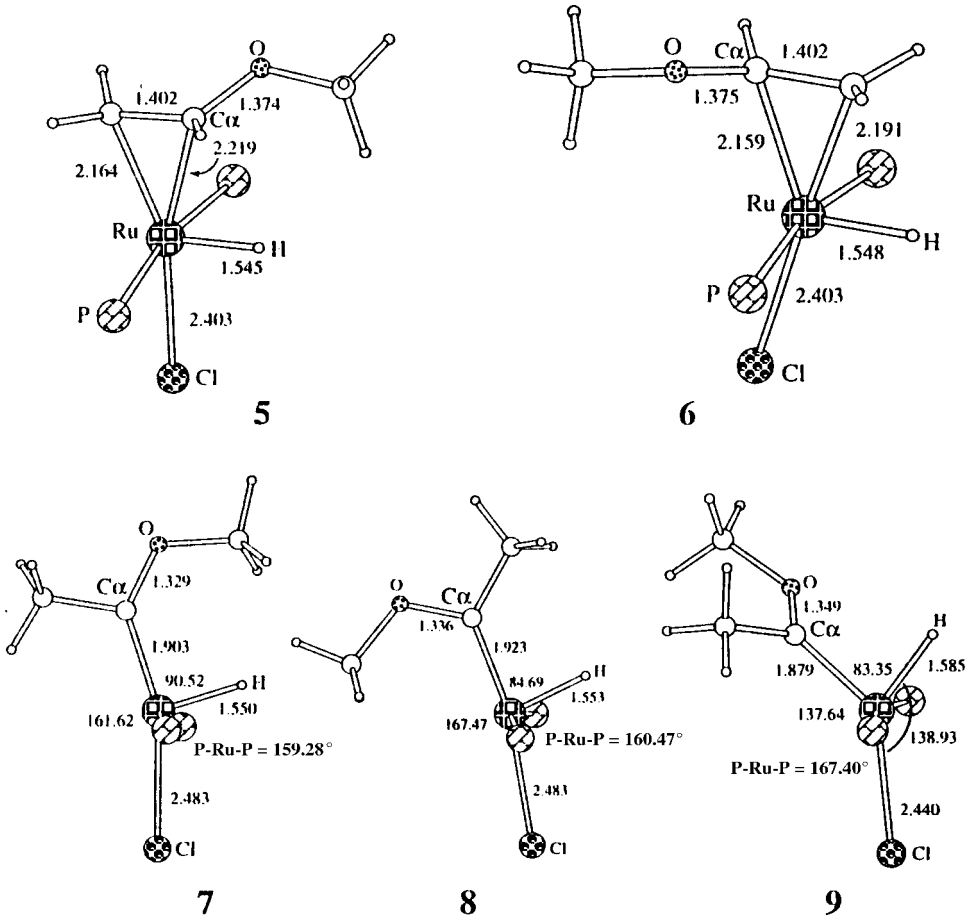

Fig. 6 DFT(B3PW91) optimized structures for isomeric $RuC_2H_4(OCH_3)Cl(PH_3)_2$ isomers.

corresponding distance in the case of an ethylene ligand (2.19 Å *vs.* 2.23 Å), consistent with the slight attraction described above. Remarkably, the Ru–olefin bond dissociation energy (BDE ≈ 39 kcal mol^{-1}) is also not affected by the presence of OCH_3 (average difference of 3.0 kcal mol^{-1} with the greater dissociation energy for ethylene). While OCH_3 certainly increases the electron-donating ability of the π system, it decreases its π-accepting capability. These two effects act in opposite directions to maintain the binding energy to the metal constant. This emphasizes that [**Ru**], although strongly electron-deficient, is not acting solely as a Lewis acid but certainly has important back-donating capabilities.

The structures of several conformations (all minima) of the [**Ru**]=C(CH_3)(OCH_3) isomer are also shown in Fig. 6. In the two most stable conformations, the carbene is in the mirror plane of the molecule. These two conformations, **7** (OCH_3 *cis* to H with respect to the Ru=C bond) and **8** (OCH_3 *trans* to H with respect to the Ru=C bond), are only 0.25 kcal mol^{-1} apart and thus at the same energy. The conformation **9** with the carbene plane perpendicular to the mirror plane is calculated to be 4.1 kcal mol^{-1} above the most stable conformation. Since **9** would be highly disfavored on steric grounds in the real system, the two preferred conformations are **7** and **8**. Finally, a carbene complex in which the oxygen would coordinate Ru (**I**) was sought as a minimum on the potential energy surface without success. Any such structure optimized to **8**. No 18-electron C- *and* O-bonded carbene complex is more stable than the 16-e unsaturated η^1-bonded C(CH_3)(OCH_3) species.

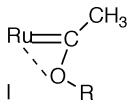

I

The preferred orientation C(CH_3)(OCH_3) is thus rotated by 90° with respect to that in **4**, the C(H)CH_3 complex. The coordination around the metal is also different for the two carbene ligands. For C(H)CH_3, ∠Cl–Ru–C is equal to 129.5° and ∠Cl–Ru–H is equal to 142.5°. With the OCH_3 substituent ∠Cl–Ru–C is 161.6° (**7**) and 167.5° (**8**), while ∠Cl–Ru–H is 107.9° or 107.8°, respectively. The coordination at the metal has thus changed from a Y shape [C(H)Me] to a T shape [C(CH_3)OCH_3]. It should be noticed that the change from Y to T shapes at Ru is associated with the rotation of the carbene and not solely with the presence of the OMe substituent. Thus, in **9** where the C(Me)(OCH_3) is perpendicular to the mirror plane, the coordination geometry at Ru is similar to that of **4**. The preference of different carbene conformations for the Y and T shape complexes has its origin in the back-bonding from Ru to the carbene. In the Y shape, as mentioned above, the highest occupied d orbital is $d_{x^2-y^2}$ resulting in a carbene perpendicular to the mirror plane. In the T structure, the d_{xy} and d_{xz} (**J**) orbitals are both destabilized by a Cl lone pair and are thus each good candidates for back-donating into carbene. An additional increase in back-bonding is caused by bending the phosphine ligands away from the carbene. This is only possible when the carbene lies perpendicular to the Ru–P bonds as in **7** or **8** so that its π orbitals can accept electrons from d_{xz}.

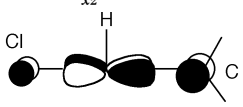

J

The OCH_3 group acts as a π donor in the carbene and not in the olefin adduct as shown by the significantly shorter C(sp^2)–O bond in the former systems. The π donation of the OCH_3 group weakens the electron donation from Ru–C as proven by the comparison of **4** and **6** or **7** and **8**, where the Ru–C_α bond is the shortest for C(H)CH_3.

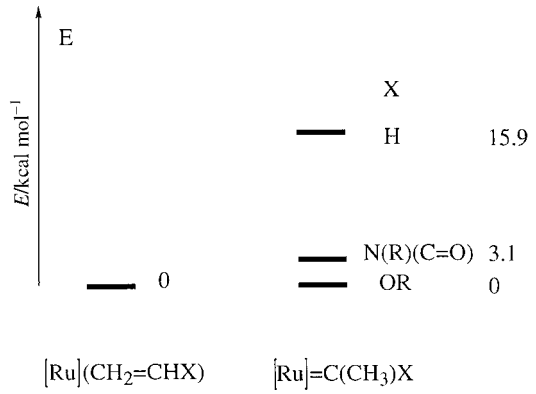

Fig. 7 Comparison of the influence of substituent X on isomer stabilities.

The presence of the π-donor group OCH_3 has also significantly decreased the difference in energy between the olefinic adduct and its carbene isomers (Fig. 7). In the case of ethylene, the isomerization was endothermic by 15.9 kcal mol^{-1}. In the case of vinyl ether, the isomerization is calculated to be essentially thermoneutral. The isomer of the carbene complex with the OMe group on C_β (**9′**) has been calculated to be 21.1 kcal mol^{-1} above the most stable olefin adduct. The difference in energy between the olefin adduct CH_2=CHX and the carbene isomer increases in the order X = OMe on C_α (0), H (15.9) OMe on C_β (21.1 kcal mol^{-1}). Thus, the OMe group greatly facilitates the formation of the isomer when positioned on C_α, but significantly disfavored the formation of carbene when on C_β. Despite the fact that the initial structure employed had O in the vicinity of Ru, the optimized geometry of structure **9′** shows that O has moved away from the metal. The carbene orientation and the coordination at Ru is similar to that of **9**. Despite the presence of unsaturation at Ru, the oxygen coordination does not bring any stabilization. In fact, angles Ru–C_α–C_β (132°) and C_α–C_β–O (115°) in **9′** open to keep O from being too close to the phosphine ligand. Thus, while coordination of olefin does not show any significant preference for having OMe at a given position (structure **5** and **6**), only **6** would lead to the carbene product.

It is especially illuminating to relate the difference in energy between the unsubstituted or substituted olefin adduct and the carbene complex to the corresponding values in the absence of [**Ru**]. Thus, *both* the Ru fragment [eqn. (14) *vs.* (16)] and the OCH_3 substituent [eqn. (14) *vs.* (15)] drastically decrease the isomerization energy of olefin into carbene since both can donate to the empty p orbital of the carbene. The competition between [**Ru**] and OCH_3 in donation to the same empty carbene p orbital results in some interesting features in the following isodesmic reactions.

$$C_2H_4 \rightarrow C(H)CH_3 \quad \Delta E = 79.1 \text{ kcal mol}^{-1} \qquad (14)$$

$$CH_2C(H)(OCH_3) \rightarrow C(CH_3)OCH_3 \quad \Delta E = 41.4 \text{ kcal mol}^{-1} \qquad (15)$$

$$[\mathbf{Ru}](C_2H_4) \rightarrow [\mathbf{Ru}]C(H)CH_3) \quad \Delta E = 15.9 \text{ kcal mol}^{-1} \qquad (16)$$

$$[\mathbf{Ru}](CH_2{=}C(H)(OCH_3)) \rightarrow [Ru](C(CH_3)OCH_3) \quad \Delta E = 1.6 \text{ kcal mol}^{-1} \qquad (17)$$

$$C_2H_4 + C(OCH_3)(CH_3) \rightarrow CH_2{=}CH(OCH_3) + C(H)(CH_3) \quad \Delta E = 37.7 \text{ kcal mol}^{-1} \qquad (18)$$

$$C_2H_4 + [\mathbf{Ru}](C(H)CH_3) \rightarrow C(H)CH_3 + [\mathbf{Ru}](C_2H_4) \quad \Delta E = 63.2 \text{ kcal mol}^{-1} \qquad (19)$$

Eqn. (18) and (19) show that OCH_3 and [**Ru**] independently stabilize the carbene isomeric form with respect to the olefinic form by large amounts. However, eqn. (20) [in comparison to eqn. (19)] shows that [**Ru**] is less efficient in stabilizing

methoxycarbene than methyl carbene. This difference could be due to the influence of OCH_3 on the olefin and/or the carbene. However, there is no significant difference in BDE to [**Ru**] for ethylene and CH_2=$CHOCH_3$ as shown by eqn. (21). Thus, [**Ru**] stabilizes the non-substituted carbene significantly better [eqn. (22)] than the $C(CH_3)(OCH_3)$. While OCH_3 diminishes the stabilizing influence of [**Ru**] to the carbene due to the fact that both are in competition to donate to the same empty orbital of the carbene, it should be emphasized that the cooperative effect of both OCH_3 and Ru is indispensable to compensate the large difference (79.1 kcal mol^{-1}) in energy between the olefin and its isomeric carbene form [eqn. (14)].

$$CH_2{=}C(H)OCH_3 + [\mathbf{Ru}](C(CH_3)OCH_3) \rightarrow C(CH_3)OCH_3 + [\mathbf{Ru}](CH_2{=}C(H)OCH_3) \quad \Delta E = 39.8 \text{ kcal mol}^{-1} \quad (20)$$

$$[\mathbf{Ru}](C_2H_4) + CH_2{=}CHOCH_3 \rightarrow [\mathbf{Ru}](CH_2{=}CHOCH_3) + C_2H_4 \quad \Delta E = 2.6 \text{ kcal mol}^{-1} \quad (21)$$

$$[\mathbf{Ru}](C(H)CH_3) + C(CH_3)OCH_3 \rightarrow [\mathbf{Ru}][(C(CH_3)OCH_3)] + C(H)CH_3 \quad \Delta E = 25.8 \text{ kcal mol}^{-1} \quad (22)$$

DFT computational study of the amido carbene complex

The amido carbene complex in which PPr^i_3 was replaced by PH_3 (**10**) was optimized with no symmetry restriction. The optimized structure is in good accord with the experimental structure (Fig. 8). All metal-to-ligand distances are close to the experimental values with the exception of Ru···O, which is 0.1 Å too long. However, the calculated Ru···O is sufficiently short (2.370 Å) to clearly indicate the presence of a Ru···O bond. The calculated geometry within the Ru–C–N–C–O moiety mimics closely the experimental values. The N center, which is calculated to be planar, is closer to the C of carbonyl (N–C = 1.382 Å) than to C_α (1.391 Å). The five-membered ring has the usual envelope shape.

The binding energy of oxygen to the metal can be estimated from the differences in energy between **10** and optimized structures with no Ru···O interaction. To save computational time, a simplified system **11** in which the five-membered pyrrole ring is truncated, has been selected. The optimized structure of **11** (Fig. 8) gives results very similar to that of **10**. This model will thus be used for further study of the system.

The structure **12**, lacking Ru···O interaction and resulting from a rotation about the C_α–N bond, was located as a minimum (Fig. 8). The energy of **12** is 8.6 kcal mol^{-1} higher than **11**. Another minimum **13** (not shown), obtained from **12** by 180° rotation about the Ru–C_α bond, was located and is calculated to be 9.8 kcal mol^{-1} above **11**. The Ru···O bond dissociation energy is thus estimated to be about 9 kcal mol^{-1}.

There are some interesting geometry changes in going from **11** to **12**. In losing the Ru···O interaction, the carbene rotates by 43° (**13** has similar geometrical features). This unusual conformation of the carbene is thus intermediate between that of $C(H)CH_3$ and $C(CH_3)(OCH_3)$. There is an apparent corre-

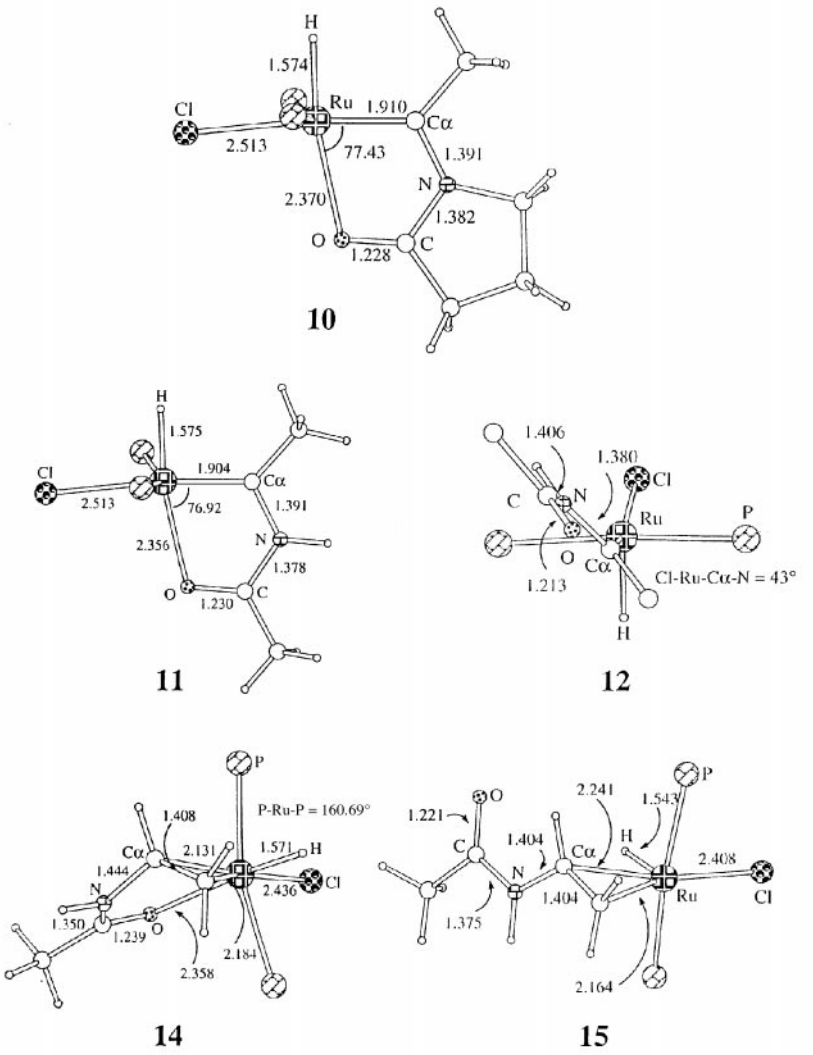

Fig. 8 DFT(B3PW91) optimized structures for $RuHCl(PH_3)_2$ with amido olefins.

lation between the donating power of the substituent on the carbene and the conformation of the carbene in the complex. We have seen that the orientation of the carbene was closely connected to the coordination geometry at the metal [Y for CHMe and T for C(OMe)(Me)]. In the case of **11** ($\angle$Cl–Ru–C_α = 162.0° and $\angle$Cl–Ru–H = 114.5°), the metal coordination is also intermediate between the $C(H)CH_3$ and $C(CH_3)OCH_3$ cases. In **12**, the nitrogen (still planar) is closer to C_α (1.380 Å) than to the C(O) carbon (1.406 Å) in contrast to **11**. The π donation of the nitrogen is thus more important towards the carbene in **12** than in **11**, due to the fact that the electron accepting ability of the acyl group is no longer enhanced by coordination to Ru.

Two olefin adducts, **14** and **15**, with a $NH(CO)(CH_3)$ substituent have been optimized. Isomer **14** is 5.5 kcal mol^{-1} more stable than **15** and has the amide oxygen coordinated to Ru with only a minor decrease in the P–Ru–P angle (160.7° in **14** and 166.6° in **15**). Thus, the more bulky phosphine used experimentally should not prevent the coordination. The proposal that O is coordinated to the metal in the olefin adduct **14** is supported by the structure of the olefin adduct of CH_2=CH(phthalimide).

The difference in energy between the most stable olefin complex **14** and the more stable carbene isomer **11** is calculated to be 3.1 kcal mol^{-1} in favor of the olefin adduct (Fig. 7). This small difference in energy, together with inclusion of steric effects (which favor the carbene over olefin complex), accounts for the fact that isomerization of the olefin substituted by the amido group has been observed. In this case, two factors contribute to make the carbene isomer energetically accessible: π donation of the nitrogen amide and coordination of the amide oxygen to Ru, which in turn probably enhances the electron-donating ability of Ru toward the carbene. It is, however, probable that π donation of the nitrogen lone pair is a major component since no isomerization is observed in the case of vinyl phthalimide.

Discussion

The multistep reaction path that is described here is analogous to that of the isomerization of terminal alkyne into vinylidene in the presence of Ru.[12] However, while the path is exothermic from the acetylene adduct to the vinylidene complex [eqn. (23)], it is endothermic in the case of ethylene [eqn. (24)]. At the heart of this is the difference in energy

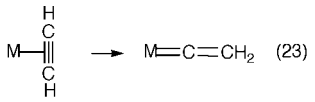

(23)

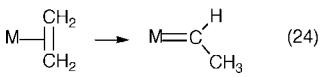

(24)

between the isomeric species [$\Delta E(C_2H_2 - C{=}CH_2) = 40$ kcal mol^{-1}][13] and [$\Delta E(C_2H_4 - C(H)CH_3) = 79.1$ kcal mol^{-1}]. This large difference, which is due to the fact that the third bond of a triple bond is much weaker than the π bond of a double bond, controls the thermochemistry of the reaction even in the presence of the metal. The presence of a π-donor group like OCH_3 lowers the endothermicity of the isomerization of free olefin to 50 kcal mol^{-1}, thus approaching that of free alkyne. Lowering the π-donating ability of the substituent on the carbene disfavors the isomerization (OMe > amide > phthalimide).

The reaction path found here for ethylene (and most likely representative of that of vinyl ether) shows the key role of the metal hydride in permiting the isomerization to occur. In the absence of the metal fragment a 1,2-shift of H in free ethylene is a very high energy process (>60 kcal mol^{-1} for propene[10] and 79.1 kcal mol^{-1}[10] for ethylene in these calculations). The presence of a transition metal complex has been shown to facilitate the 1,2 shift in the case of alkyne to vinylidene.[14] Our calculations have shown that the multistep reaction initiated by alkyne insertion into the Ru–H bond is considerably lower in energy than the 1,2 shift. In the case of olefin, the 1,2 shift, even if also facilitated by the metal, should remain energetically inaccessible. The presence of an additional H on the metal is thus indispensable for the isomerization process.

The pathway presented here also explains the isotope labeling observation with C_2D_4. The isotope scrambling is explained by the olefin adduct *entering* the hydride migration path, even if accumulation of the carbene complex is not thermodynamically possible.

Since the final complex is unsaturated, a study of the effect of an electron-donating group remote from the olefinic function has been studied. It was hoped that this would stabilize the final carbene by coordination to the unsaturated site. With the exception of the amide function where the O is positioned in close proximity to the metal and thus has been shown to coordinate, it has been observed that a more remote functionality does not interact with the metal. This illustrates the relatively poor Lewis acidity of Ru with a hydride *trans* to the empty site.

The chemistry of transition metal carbene complexes, $L_nMC(X)R$ (*i.e.*, terminal carbenes) has been categorized into two types, named after their discoverers as Fischer carbenes and Schrock carbenes. As outlined in a recent theoretical study,[15] these are conventionally distinguished by a low metal oxidation state and X a π donor (OR′, NR'_2, *etc.*) for Fischer carbenes, and a high metal oxidation state and X a pure sigma ligand (H, alkyl, silyl, *etc.*) for Schrock carbenes. In our case, is a Ru(II) complex of a carbene with a π-donor group $RuHCl(C(OR)R')L_2$ and no CO ligands a Fischer- or a Schrock-type carbene? These mentioned "distinguishing features" fail to recognize two other differences. (1) Fischer carbene complexes generally have the strong π acid CO for some or all of the co-ligands L (which will tend to minimize M → CXR back-bonding and thus put higher demands on X → C π bonding) while Schrock carbenes have strong sigma donors (alkyls and phosphines) and sometimes π donors (alkoxides) for L. (2) Fischer carbene complexes invariably have an 18-electron count at M while Schrock carbene complexes generally have 16 or fewer valence electrons. In short, it is unreasonable that the overall differences are based primarily on the MC(X)R substructure; the identity of L and the value of *n* in $L_nMC(X)R$ are important, and perhaps controlling factors.

Above and beyond this analysis of differences, a distinction between Fischer and Schrock carbenes is that the former *react* with the carbene carbon behaving like an electrophile, while Schrock carbenes *react* with the carbene carbon behaving like a nucleophile. It is thus paradoxical that the *low* oxidation state metal promotes electrophilic carbene character, since an electron-rich metal should maximize back donation. Likewise, a high metal oxidation state should *not* cause a nucleophilic carbene carbon. Moreover, it is also irrational that a π-donor substituent on the carbene carbon should leave that carbene *electrophilic*.

In addition, exceptions exist to the above systematics. $Cp_2Ta(CH_3)(CH_2)$ does *not* show Wittig reactivity under mild conditions. $W(CPh_2)(CO)_5$ does not effect olefin metathesis until one CO is displaced, from which we can conclude that olefin metathesis requires prior W–olefin bonding and does not proceed from direct contact between the carbene carbon and an olefin. Indeed, it is not at all established that olefin metathesis benefits from nucleophilic *vs.* electrophilic carbene carbon character. These characteristics may in fact be quite irrelevant.

Reactivity is not necessarily a reflection of the character of an unperturbed molecule. In particular, the Wittig-like reactivity of certain Schrock carbenes [eqn. (25), which is a prime source for the claim of nucleophilic carbon character in Schrock carbenes] probably originates from an adduct **K** in which the acetone carbon is made more electrophilic by Ta and such substrate binding also makes C′ more nucleophilic.

$$R_3TaCHR + Me_2CO \rightarrow \text{“}R_3TaO\text{”} + RHC{=}CMe_2 \quad (25)$$

The unsaturation at M is probably a key factor in the reactivity dichotomy between Fischer and Schrock carbenes. In support of this assertion, a theoretical study[15] has revealed how addition of one fluoride to the Schrock carbene model F_4WCH_2 to give $F_5WCH_2^-$, alters the W–CH_2 bond to something that resembles the same bond in $(OC)_5WCH_2$. Indeed, Roper and colleagues long ago noted that oxidation state is not a safe criterion for predicting electrophilic or nucleophilic reactivity.[16] Two related $CpRe(CO)_2(CRR')$ species are susceptible to both electrophilic and nucleophilic addition to the carbene carbon; when R is OEt, electrophilic addition (*i.e.*, H^+) no longer occurs.[17] Thus, metal oxidation state is not a controlling factor, and unsaturation at the metal is a key (but not sufficient) factor. In this context, the ruthenium chemistry reported here illustrates a class of compounds that fit neither traditional carbene complex category. $RuHCl[C(OR)R']L_2$ carries a π-donor substituent on the carbene carbon, the metal is in an intermediate oxidation state [but Ru(II) is a fairly powerful π base], but the metal is unsaturated.

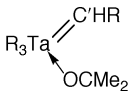

Several theoretical studies using GVB, NBO and CDA analyses have been carried out on representative selections of carbene complexes to classify the carbene complexes as a member of *either* Fischer or Schrock series.[15] With these tools, Fischer carbenes were shown to be donor-acceptor complexes involving metal and carbene fragments in a singlet state, while the Schrock carbenes should be discussed in terms of interactions between metal and carbene fragments in the triplet states. If in fact the energy gap between singlet and triplet of each fragment is a controlling criterion, there is no reason to partition into two classes, as a continuum situation is highly probable. This is probably the right time to recognize that there will be a continuum of carbene “characters”, and to cease trying to place new ones in *either* the Fischer *or* the Schrock category.[17] The systems presented here offer an ideal study ground for a more in-depth understanding of what controls the changes from Fischer to Schrock carbenes. The presence of unsaturation and the nature of the ligand *trans* to the empty site are probably key factors that have not been noticed earlier.

A CDA analysis[15] was carried out on several representative 16-electron carbene complexes resulting from union of the fragments $RuXY(PH_3)_2$ and $CH(CH_3)$ or $C(OCH_3)(CH_3)$. As shown by this analysis, a Fischer complex is characterized by a large carbene → metal donation (large positive *d*), a large metal → carbene back donation (large positive *b*), a large repulsive polarization (large negative *r*) and a small residual ε. Schrock complexes are characterized mostly by large residual and small *d*, *b* and *r*. These values have been calculated (Table 5) for $RuHCl(PH_3)_2(CH(CH_3))$, $RuHCl(PH_3)_2(C(OCH_3)(CH_3))$ in the three minima (**7**, **8** and **9**) and for $RuCl_2(PH_3)_2(CH(CH_3))$ as a reference system. The parameter values show that the OCH_3 substituted carbenes are ideal Fischer carbenes, especially in the two most stable conformations (**7** and **8**); conformation **9** has a slightly higher residual but is still clearly a Fischer carbene. $RuCl_2(PH_3)_2[CH(CH_3)]$ is a typical Schrock complex with a large residual (0.325) and very small *d*, *b* and *r* values. Changing Cl into H on the metal gives a species that has reasonable *d*, *b* and *r* values but a non-negligible residual. It is thus remarkable that the same metal fragment with the same formal oxidation state can result in carbene complexes with a continuum of behavior between Fischer and Schrock types. This is probably associated with a metal fragment having a singlet-triplet gap highly sensitive to the nature of the substituent. This is apparently a very remarkable feature of the 14-electron $RuXYL_2$ fragments.

The isomerization reaction type observed here seems quite general for vinyl ethers; it demonstrates that the hydrido carbene is more stable thermodynamically than either the hydrido olefin or the alkyl isomer [eqn. (26)] and it shows that there is no tendency for the hetero substituent on the carbene to diminish the unsaturation at Ru by direct O → Ru binding. Isotope labeling using CH_2=CD(OEt) and DFT calculations both prove that the regiochemistry of addition of Ru–H across the H_2C=CH(OR) bond is not selective, but that only the direction shown in eqn. (26) leads to the thermodynamically preferred carbene. The alternative intermediate [eqn. (27)] leads to a carbene devoid of heteroatom stabilization, which is apparently thermodynamically less stable.

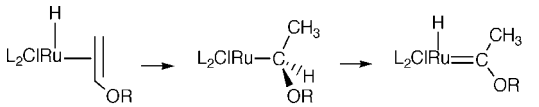

(26)

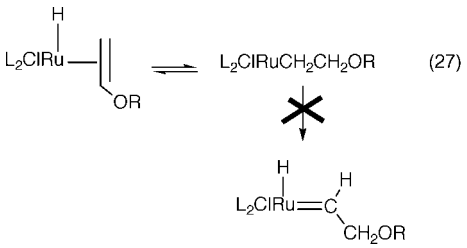

(27)

Why has this facile isomerization route to carbene ligands not already been discovered? First, the organometallic chemistry of vinyl ethers has not been extensively investigated in modern times,[18,19] and what has been done centers on electrophilic attack on the ether oxygen (*i.e.*, RO^- abstraction, to give vinyl complexes) of less electron-rich, and saturated molecules. More important, previous reports involved nonhydride compounds, which are thus unable to effect the mechanism established here. Finally, any previous study under hydrogen gas, even if it involved carbene intermediates, would have given an alkane product since the *unsaturated* carbenes of the sort produced here are readily hydrogenated to alkanes [eqn.

Table 5 CDA analysis from DFT wavefunctions

	d	*b*	*r*	ε
$(H_3P)_2RuHCl[CH(CH_3)]$	0.335	0.273	−0.287	0.117
$(H_3P)_2RuHCl[C(OMe)(CH_3)]$, **9**	0.470	0.264	−0.323	0.058
$(H_3P)_2RuHCl[C(OMe)(CH_3)]$, **7** or **8**	0.487	0.314	−0.425	0.000
$(H_3P)_2RuCl_2[CH(CH_3)]$	0.003	0.058	0.008	0.325

(28); 1 atm H_2, C_6D_6, 60 min at 25 °C]. To answer the question that begins this paragraph, a referee has commented that "It has, in a way . . . " In a previous report,[20] the thermodynamic preference for ethylidene in the isomerization of ethylene on a highly reducing $(Me_3SiNC_2H_4)_3NTa$ fragment, was attributes to an α-agostic interaction.

$$ClHL_2Ru{=}C(Me)(OEt) + 2\ H_2 \rightarrow RuH_3ClL_2 + Et_2O \quad (28)$$

The implication of the above is that *any* unsaturated *mono*-hydride has the potential to effect this carbene synthesis from vinyl ethers. To be able to do this, the chosen metal must be sufficiently electron-rich to tolerate the higher formal oxidation state of the carbene product. In practice, however, we have found that $OsHCl(PPh_3)_3$ can be stirred in C_6H_6 with equimolar $H_2C{=}CH(OR)$ (R = Et or Bu^t) at 25 °C for up to 90 h without change. With $RuHCl(PPh_3)_3$ there is no reaction with ethyl vinyl ether over 3 days at 60 °C in C_6D_6. We continue to search for other unsaturated monohydrides capable of this isomerization, with special attention to whether a 14-electron configuration and/or a four-coordinate structure is a necessity.

There is a general belief that Fischer carbenes are "more stable" than Schrock carbenes, and this is attributed to π donation by the heteroatom to the carbene carbon. Quantitative comparison of "stability" is however *not* established in such commentaries since there are no isomeric forms for experimental comparison. Instead, the discussion usually hinges on Fischer carbenes having an electrophlic carbon while Schrock carbenes have nucleophilic carbon; these have no direct relation to "stability". What the calculations reveal here on the systems studied experimentally is that, for isomeric alternative carbenes on Ru, the heteroatom on the carbene carbon is indeed more stable. *Via* the thermodynamic cycles in Scheme 2, this can be traced primarily to the properties of the free carbenes [$\Delta E(\alpha \rightarrow \beta)$ *vs.* $\Delta E(\beta \rightarrow \alpha)$ to make the two different carbenes]. The heteroatom makes the carbene more stable (more energetically accessible). Since this is close to the calculated difference in overall $\Delta E(1)$ and $\Delta E(2)$, it follows that the two BDEs do not differ greatly. That is, differences in the bonding of the two isomeric carbenes to Ru are less important than the differences in the energies of the *free* carbenes themselves. Thus, no comparative conclusions can be drawn, from the observed isomerization, about the Ru=C bond. The formation of the heteroatom carbene is possible due to properties of the metal-free hydrocarbon isomers.

Experimental

Computational details

Ab initio calculations were carried out with the Gaussian 94[21] set of programs within the framework of DFT at the B3PW91 level.[22] The Hay–Wadt effective core potential (quasi-relativistic for the metal centers) was used to replace the 28 innermost electrons of Ru[23] and the 10 core electrons of P and Cl.[24] The associated double ζ basis sets were used. They were augmented by d polarization functions for P and Cl.[25] H, C, O and N were represented by a 6-31G(d,p) basis set.[26] In the case of the olefin substituted by an amide group (**10**), a STO-3G basis set was used for the CH_2 group of the five-membered ring as well as the H of PH_3. Comparison between the results with the smaller basis set and the larger one (as defined above) for **11** proved the more restricted basis set to give good geometrical results. Full geometry optimization was performed without symmetry restriction. For the reaction path of isomerization of the C_2H_4 adduct into the $C(H)CH_3$ complex, the nature of the optimized structure as a minimum or a transition state was checked by numerical frequency calculations. The transition-state structures were given small geometrical perturbations along the reaction coordinates and then further geometrical optimization was carried out to ensure they connect the reactant and product of interest.

Syntheses and reactions

All manipulations were performed using standard Schlenk techniques or in an argon-filled glovebox unless otherwise noted. Solvents were distilled from Na/benzophenone or CaH_2, degassed prior to use, and stored in air-tight vessels. Commercially available vinyl ethers, amines and amides were used as received after drying and degassing. ^1H NMR chemical shifts are reported in ppm relative to protio impurities in the deutero solvents. ^{31}P and ^{19}F NMR spectra are referenced to external standards of 85% H_3PO_4 and $CFCl_3$, respectively (both at 0 ppm). NMR spectra were recorded with either Varian GEMINI 2000 (300 MHz ^1H; 121 MHz ^{31}P; 75 MHz ^{13}C; 282 MHz ^{19}F) or Varian UNITY INOVA (400 MHz ^1H; 162 MHz ^{31}P; 101 MHz ^{13}C; 376 MHz ^{19}F) instruments. IR spectra were recorded on a Nicolet 510P FT-IR spectrometer equipped with OMNIC v.4.1b software.

Preparation of $RuHCl(PPr^i_3)_2$. Under Ar, 750 mg (1.64 mmol) of $RuH_2Cl_2(PPr^i_3)_2$[27] and 230 mg (1.64 mmol) of lithium 2,2,6,6-tetramethylpiperidide were added to a Schlenk flask equipped with a stir bar. Approximately 25 mL of pentane was added and the reaction allowed to stir overnight. The solution was filtered thought a medium porosity frit and the solvent was removed to a liquid N_2 trap. The deep red product was dried *in vacuo* overnight to yield 510 mg of $RuHCl(PPr^i_3)_2$ (73%). The compound can be heated mildly (55 °C) to facilitate removal of the free amine generated and can also be washed with small portions of hexamethyldisiloxane if necessary. ^1H NMR (400 MHz, C_6D_6, 20 °C): δ −24.2 (t, $^2J_{P\text{-}H} = 32.8$ Hz, Ru*H*), 1.34 [dvt, $J_{P\text{-}H} = {}^3J_{H\text{-}H} = 6.2$ Hz, 18H, $P(CHMe_2)_3$], 1.36 [dvt, $J_{P\text{-}H} = {}^3J_{H\text{-}H} = 6.2$ Hz, 18H, $P(CHMe_2)_3$], 2.19 [m, 6H, $P(CHMe_2)_3$]. $^{31}P\{^1H\}$ NMR (162 MHz, C_6D_6, 20 °C): δ 84.1 (s). $^{13}C\{^1H\}$ NMR (75.5 MHz, C_6D_6, 20 °C): δ 20.8 [s, $P(CHMe_2)_3$], 21.2 [s, $P(CHMe_2)_3$], 28.4 [vt, $J_{P\text{-}C} = 6.4$ Hz, $P(CHMe_2)_3$].

$RuHCl(PPr^i_3)_2(N_2)$. Under Ar, 15 mg (0.033 mmol) $RuHCl(PPr^i_3)_2$ in 0.5 mL benzene-d_6 was added to an NMR tube equipped with a Teflon stopcock. The sample was degassed, the benzene frozen in ice, and the tube filled to

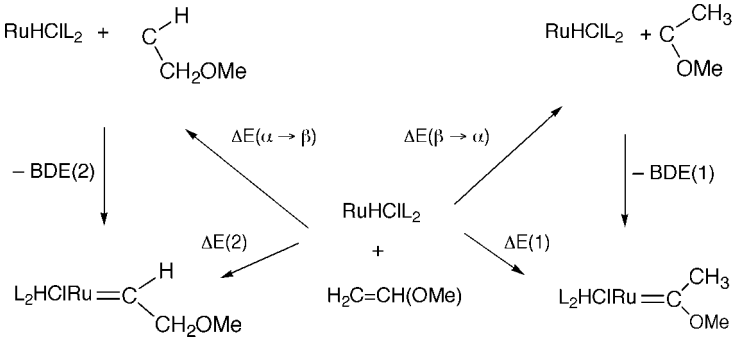

Scheme 2

approximately 1 atm with N_2. Agitation of the tube resulted in complete conversion to the dinitrogen adduct within 5 min. ^{1}H NMR (300 MHz, C_6D_6, 20 °C): δ −28.1 (t, $^2J_{P-H}$ = 18.3 Hz, Ru*H*), 1.22 [dvt, $J_{P-H} = {}^3J_{H-H}$ = 6.6 Hz, 18H, P(CH*Me*$_2$)$_3$]), δ 1.24 [dvt, $J_{P-H} = {}^3J_{H-H}$ = 6.6 Hz, 18H, P(CH*Me*$_2$)$_3$], 2.56 [br s, 6H, P(C*H*Me$_2$)$_3$]. ^{31}P{^{1}H} NMR (121 MHz, C_6D_6, 20 °C): δ 55.6 (s).

RuHCl(PPr$^i_3$)$_2$(C$_5$H$_5$N). Under Ar, 10 mg (0.022 mmol) RuHCl(PPr$^i_3$)$_2$ was dissolved in 0.5 mL C_6D_6, 1.8 μL (0.022 mmol) pyridine is added and the tube shaken. Conversion to the pyridine adduct was complete in the time of mixing as evidenced by a color change from dark red to bright red-orange. ^{1}H NMR (400 MHz, C_6D_6, 20 °C): δ −20.9 (t, $^2J_{P-H}$ = 24.4 Hz, 1H, Ru*H*), 1.38 [dvt, $J_{P-H} = {}^3J_{H-H}$ = 6.4 Hz, 36H, P(CH*Me*$_2$)$_3$, both diastereotopic methyl groups are seen as a single signal from coincidental overlap], 1.71 [m, 6H, P(C*H*Me$_2$)$_3$], 6.02 (apparent t, $^3J_{H-H}$ = 6.0 Hz, 1H, C_5H_5N), 6.26 (apparent t, $^3J_{H-H}$ = 6.0 Hz, 1H, C_5H_5N), 6.56 (apparent t, $^3J_{H-H}$ = 7.4 Hz, 1H, C_5H_5N), 8.94 (d, $^3J_{H-H}$ = 5.6 Hz, 1H, C_5H_5N), 10.74 (d, $^3J_{H-H}$ = 5.6 Hz, 1H, C_5H_5N). ^{31}P{^{1}H} NMR (162 MHz, C_6D_6, 20 °C): δ 37.9 (s). ^{13}C{^{1}H} NMR (101 MHz, C_6D_6, 20 °C): δ 20.3 [s, P(CH*Me*$_2$)$_3$], 20.8 [s, P(CH*Me*$_2$)$_3$], 25.4 [vt, J_{P-C} = 6.0 Hz, P(*C*HMe$_2$)$_3$], 120.7 (s, *C*$_5$H$_5$N), 121.9 (s, *C*$_5$H$_5$N), 132.2 (s, *C*$_5$H$_5$N), 160.5 (s, *C*$_5$H$_5$N), 163.1 (s, *C*$_5$H$_5$N).

RuHCl(PPr$^i_3$)$_2$ with 2 C$_5$H$_5$N. Under Ar, 10 mg (0.022 mmol) RuHCl(PPr$^i_3$)$_2$ was dissolved in 0.5 mL C_6D_6, 3.6 μL (0.044 mmol) pyridine added and the tube shaken. After 10 min ^{1}H and ^{31}P{^{1}H} NMR revealed the generation of a mixture of RuHCl(PPr$^i_3$)$_2$(C$_5$H$_5$N) (above), RuHCl(PPr$^i_3$)$_2$(C$_5$H$_5$N)$_2$, and RuHCl(PPr$^i_3$)(C$_5$H$_5$N)$_2$, as well as the presence of free phosphine. **RuHCl(PPr$^i_3$)$_2$(C$_5$H$_5$N)$_2$:** ^{1}H NMR (400 MHz, C_6D_6, 20 °C): δ −12.9 (t, $^2J_{P-H}$ = 14 Hz, Ru*H*). ^{31}P{^{1}H} NMR (162 MHz, C_6D_6, 20 °C): δ 56.1 or 71.0 (s). **RuHCl(PPr$^i_3$)(C$_5$H$_5$N)$_2$:** ^{1}H NMR (400 MHz, C_6D_6, 20 °C): δ −20.0 (d, $^2J_{P-H}$ = 30 Hz, Ru*H*). ^{31}P{^{1}H} NMR (162 MHz, C_6D_6, 20 °C): δ 71.0 or 56.1 (s).

RuHCl(PPr$^i_3$)$_2$(CH$_2$=CH$_2$). Under Ar, 10 mg (0.022 mmol) RuHCl(PPr$^i_3$)$_2$ was added to an NMR tube equipped with a Teflon stopcock. The tube was filled with C_6D_6 to a predetermined mark on the tube so that the remaining head space volume was 4.0 mL (approximately 0.5 mL C_6D_6). The NMR tube was cooled to 0 °C to freeze the benzene-d_6 and was then evacuated. It was then filled with ethylene (0.022 mmol) to 95 mm Hg and the stopcock closed. The sample was then warmed to room temperature, shaken, and its ^{1}H and ^{31}P{^{1}H} NMR spectra taken over 30 min intervals. The adduct that formed showed little or no decomposition over a period of several hours. ^{1}H NMR (400 MHz, C_6D_6, 20 °C): δ −22.0 (t, $^2J_{P-H}$ = 18.0 Hz, Ru*H*), 1.15 [dvt, $J_{P-H} = {}^3J_{H-H}$ = 6.0 Hz, 18H, P(CH*Me*$_2$)$_3$], 1.20 [dvt, $J_{P-H} = {}^3J_{H-H}$ = 6.0 Hz, 18H, P(CH*Me*$_2$)$_3$], 2.25 [m, 6H, P(C*H*Me$_2$)$_3$], 2.79 [t, $^4J_{P-H}$ = 3.2 Hz, 4H, Ru(C*H*$_2$=C*H*$_2$)]. ^{31}P{^{1}H} NMR (162 MHz, C_6D_6, 20 °C): δ 44.1 (s).

Reaction of RuHCl(PPr$^i_3$)$_2$ with CD$_2$=CD$_2$. Reversible insertion. Under Ar, 10 mg (0.022 mmol) RuHCl(PPr$^i_3$)$_2$ was added to an NMR tube equipped with a Teflon stopcock in 0.5 mL of benzene. The tube was frozen in ice, evacuated, and CD_2=CD_2 (600 torr) was added. ^{2}H NMR (20 °C) spectra taken after 1 h at room temperature show deuterium incorporation into the PPr$^i_3$ methyl groups (δ 1.2), and into the hydride position (δ −22.0) in addition to being present in the olefinic adduct (δ 2.8). This is indicative of reversible insertion of the ethylene unit into the Ru–H bond.

RuHClL$_2$ with 1-hexene or styrene. Under argon, 10.0 mg (0.022 mmol) RuHClL$_2$ was dissolved in 0.5 mL C_6D_6 in an NMR tube and 2.8 μL (0.022 mmol) 1-hexene or 2.5 μL (0.022 mmol) styrene added. In each case, after 30 min, an olefin adduct was observed in approximately 10% population relative to unreacted RuHClL$_2$, though longer reaction times lead to an unidentified mixture of products. The olefinic protons of the adduct were not resolved due to coincidental overlap with the PPr$^i_3$ ligands. **RuHClL$_2$(CH$_2$=CHC$_4$H$_9$).** ^{1}H NMR (400 MHz, benzene-d_6): δ −23.7 (m, 1H, Ru*H*). ^{31}P{^{1}H} NMR (162 MHz, benzene-d_6): δ 34.9, 39.5 (AB pattern, $^2J_{P-P}$ = 287 Hz). **RuHClL$_2$(CH$_2$=CHPh).** ^{1}H NMR (400 MHz, benzene-d_6): δ −22.1 (apparent t, $^2J_{H-P}$ = 34 Hz, 1H, Ru*H*). ^{31}P{^{1}H} NMR (162 MHz, benzene-d_6): δ 85.3, 86.4 (AB pattern, $^2J_{P-P}$ = 34 Hz).

RuHCl(PPr$^i_3$)$_2$=C(Me)OEt. Under Ar, 25 mg (0.055 mmol) of RuHCl(PPr$^i_3$)$_2$ was placed in an NMR tube in C_6D_6. *Via* syringe, 5.2 μL (0.055 mmol) of ethyl vinyl ether was added and the NMR tube sealed. ^{1}H, ^{13}C{^{1}H}, and ^{31}P{^{1}H} NMR spectra taken after approximately 30 min revealed quantitative conversion to RuHCl(PPr$^i_3$)$_2$(=C(Me)OEt). The complex can be isolated as an orange-brown viscous oil from benzene if a larger quantity is required. ^{1}H NMR (300 MHz, C_6D_6, 20 °C): δ −21.65 (t, $^2J_{P-H}$ = 22.8 Hz, 1H, Ru*H*), 1.13 [dvt, $J_{P-H} = {}^3J_{H-H}$ = 6.3 Hz, 18H0, P(CH*Me*$_2$)$_3$], 1.25 [dvt, $J_{P-H} = {}^3J_{H-H}$ = 6.3 Hz, 18H, P(CH*Me*$_2$)$_3$], 1.17 [t, $^3J_{H-H}$ = 7.2 Hz, 3H, Ru**2**C(Me)OCH$_2$C*H*$_3$], 2.33–2.44 [m, 6H, P(C*H*Me$_2$)$_3$], 2.69 [s, 3H, Ru=C(*Me*)OEt], 4.37 [q, $^3J_{H-H}$ = 7.5 Hz, 2H, Ru=C(Me)OC*H*$_2$CH$_3$]. ^{31}P{^{1}H} NMR (121 MHz, C_6D_6, 20 °C): δ 58.2 (s). ^{13}C{^{1}H} NMR (75.5 MHz, C_6D_6, 20 °C): δ 14.6 [s, Ru=C(Me)OCH$_2$*C*H$_3$], 19.7 [s, P(CH*Me*$_2$)$_3$], 20.4 [s, P(CH*Me*$_2$)$_3$], 26.2 [vt, J_{P-C} = 9.1 Hz, P(*C*HMe$_2$)$_3$], 40.8 [s, Ru=C(*Me*)OEt], 68.5 [s, Ru=C(Me)O*C*H$_2$CH$_3$], 289.8 [t, $^2J_{P-C}$ = 9.7 Hz, Ru=*C*(Me)OEt].

Upon cooling a sample of RuHCl(PPr$^i_3$)$_2$(=C(Me)OEt) in toluene-d_8 to −90 °C, slowed rotation of the ruthenium carbene bond allowed detection of the two isomers, which differ in *E*/*Z* stereochemistry about the (X)(Y)Ru=CRR′ bond. ^{1}H NMR (400 MHz, toluene-d_8, −80 °C): New signals were seen at δ 4.95 and 4.29 [1 : 10 ratio, coalesced to the time-averaged signal at δ 4.38, Ru=C(Me)OC*H*$_2$CH$_3$], δ 2.06 and 2.87 (1 : 10 ratio, coalesce at δ 2.68, Ru=C(*Me*)OCH$_2$CH$_3$], and δ −25.38 and −21.29 (1 : 10 ratio, coalesce at δ −21.68, Ru*H*). ^{31}P{^{1}H} NMR (162 MHz, toluene-d_8, −80 °C): δ 51.8 and 56.4 (1 : 10 ratio, coalesce at δ 56.0).

Detection of RuHCl(PPr$^i_3$)$_2$(CH$_2$CHOEt). Low temperature adduct. Under Ar, RuHCl(PPr$^i_3$)$_2$ (10 mg, 0.022 mmol) was dissolved in toluene-d_8 (*ca.* 0.5 mL) in an NMR tube equipped with a Teflon stopcock. Ethyl vinyl ether (2.0 μL, 0.022 mmol) was then added to the NMR tube such that it did not mix with the toluene-d_8 solution. The sample was then cooled in a dry ice–isopropanol bath, shaken to thoroughly mix the reagents and placed immediately in a pre-cooled (−85 °C) NMR spectrometer probe. The probe temperature was subsequently raised in 10 °C increments (allowing 10 min to stabilize at each interval) and the ^{1}H and ^{31}P{^{1}H} spectra were recorded. Selected NMR spectroscopic data for RuHCl(PPr$^i_3$)$_2$(CH$_2$=CHOEt) follows. The olefinic protons of the adduct were not resolved due to coincidental overlap with the PPr$^i_3$ ligands. ^{1}H NMR (300 MHz, toluene-d_8): δ −15.52 (t, $^2J_{P-H}$ = 17.7 Hz, 1H, Ru*H*), 3.69 [m, 1H, Ru(CH$_2$=CHOC*H*$_2$CH$_3$)], 4.35 [m, 1H, Ru (CH$_2$=CHOC*H*$_2$CH$_3$)], 2.02 [m, 3H, P(C*H*Me$_2$)$_3$], 2.32 [m, 3H, P(C*H*Me$_2$)$_3$]. ^{31}P{^{1}H} NMR (121 MHz, toluene-d_8): δ 40.8, 46.0 (AB pattern, $^2J_{P_A-P_B}$ = 300 Hz).

Hydrogenation of RuHClL$_2$(=C(OEt)Me). Under argon, 10.0 mg (0.022 mmol) RuHClL$_2$ was dissolved in 0.5 mL C_6D_6 in an NMR tube equipped with a Teflon stopcock and

2.4 μL (0.022 mmol) ethyl vinyl ether added. After formation of the carbene, as verified by ^{31}P NMR, the solution was frozen in ice, the headspace gases removed, and the tube filled to 1 atm with H_2. After 30 min at room temperature, over 50% conversion of $RuHClL_2$(=C(OEt)Me) to RuH_3ClL_2 [28] and diethyl ether was achieved.

RuHCl(PPr$^i_3$)$_2$(COCH$_2$CH$_2$CH$_2$). Under Ar, 25 mg (0.055 mmol) $RuHCl(PPr^i_3)_2$ was added to an NMR tube in C_6D_6. *Via* syringe, 4.2 μL (0.055 mmol) of 2,3-dihydrofuran was added and the tube sealed. After 30 min NMR spectra were recorded. The benzene-d_6 was then removed to a −196 °C trap, the product was re-dissolved in CD_2Cl_2, and the ^{1}H spectra measured again to resolve all peaks. In C_6D_6, the central methylene unit of the carbene substituent was not resolved. ^{1}H, ^{13}C{^{1}H}, and ^{31}P{^{1}H} NMR showed quantitative conversion to $RuHCl(PPr^i_3)_2$(=COCH$_2$CH$_2$CH$_2$). ^{1}H NMR (300 MHz, CD_2Cl_2, 20 °C): δ −18.20 (t, $^2J_{P\text{-}H}$ = 21.9 Hz, 1H, Ru*H*), 1.19 [dvt, $J_{P\text{-}H} = {}^3J_{H\text{-}H}$ = 6.3 Hz, 18H, P(CH*Me*$_2$)$_3$], 1.21 [dvt, $J_{P\text{-}H} = {}^3J_{H\text{-}H}$ = 6.3 Hz, 18H, P(CH*Me*$_2$)$_3$], 1.76 (apparent quintet, $^3J_{H\text{-}H}$ = 7.3 Hz, 2H, Ru=COCH$_2$C*H*$_2$CH$_2$), 2.27–2.34 [m, 6H, P(C*H*Me$_2$)$_3$], 3.07 (t, $^3J_{H\text{-}H}$ = 7.7 Hz, 2H, Ru=COCH$_2$CH$_2$C*H*$_2$), 4.19 (t, $^3J_{H\text{-}H}$ = 6.9 Hz, 2H, Ru=COC*H*$_2$CH$_2$CH$_2$). ^{31}P{^{1}H} NMR (121 MHz, C_6D_6, 20 °C): δ 60.1 (s). ^{13}C{^{1}H} NMR (75.5 MHz, C_6D_6, 20 °C): δ 20.5 [s, P(CH*Me*$_2$)$_3$], 20.8 [s, P(CH*Me*$_2$)$_3$], 24.0 (s, Ru=COCH$_2$*C*H$_2$CH$_2$), 25.5 [vt, $J_{P\text{-}C}$ = 9.4 Hz, P(*C*HMe$_2$)$_3$], 51.4 (s, Ru=COCH$_2$CH$_2$*C*H$_2$), 76.0 (s, Ru=CO*C*H$_2$CH$_2$CH$_2$), 286.6 (t, $^2J_{P\text{-}C}$ = 9.4 Hz, Ru=*C*OCH$_2$CH$_2$CH$_2$).

RuHCl(PPr$^i_3$)$_2$(=C(Me)OC$_6$H$_{11}$). Under Ar, 10 mg (0.022 mmol) of $RuHCl(PPr^i_3)_2$ was placed in an NMR tube in C_6D_6. *Via* syringe, 3.1 μL (0.022 mmol) of cyclohexyl vinyl ether was added and the tube sealed. ^{1}H and ^{31}P{^{1}H} NMR spectra taken after 1 h showed complete conversion to $RuHCl(PPr^i_3)_2$(=C(Me)OC$_6$H$_{11}$). ^{1}H NMR (400 MHz, C_6D_6, 20 °C): δ −19.39 (t, $^2J_{P\text{-}H}$ = 22.8 Hz, 1H, Ru*H*), 1.21 [dvt, $J_{P\text{-}H} = {}^3J_{H\text{-}H}$ = 6.4 Hz, 18H, P(CH*Me*$_2$)$_3$], 1.33 [dvt, $J_{P\text{-}H} = {}^3J_{H\text{-}H}$ = 6.4 Hz, 18H, P(CH*Me*$_2$)$_3$], 1.03–1.75 [m, 10H, Ru=C(Me)OC$_6$*H*$_{11}$], 2.40–2.49 [m, 6H, P(C*H*Me$_2$)$_3$], 2.72 [s, 3H, Ru=C(*Me*)OC$_6$H$_{11}$], 4.38–4.46 [m, 1H, Ru=C(Me)OC$_6$*H*$_{11}$]. ^{31}P{^{1}H} NMR (162 MHz, C_6D_6, 20 °C): δ 57.4 (s).

RuHCl(PPr$^i_3$)$_2$(=C(Me)OSiMe$_3$). Under Ar, 20 mg (0.044 mmol) of $RuHCl(PPr^i_3)_2$ was placed in an NMR tube in C_6D_6. *Via* syringe, 6.7 μL (0.044 mmol) of vinyloxytrimethylsilane was added and the tube sealed. ^{1}H, ^{13}C{^{1}H}, and ^{31}P{^{1}H} NMR spectra taken after 2 h revealed quantitative conversion to $RuHCl(PPr^i_3)_2$(=C(Me)OSiMe$_3$). ^{1}H NMR (400 MHz, C_6D_6, 20 °C): δ −17.96 (t, $^2J_{P\text{-}H}$ = 22.0 Hz, 1H, Ru*H*), 0.03 [s, 9H, Ru=C(Me)OSi*Me*$_3$], 1.24 [dvt, $J_{P\text{-}H} = {}^3J_{H\text{-}H}$ = 6.4 Hz, 18H, P(CH*Me*$_2$)$_3$], 1.27 [dvt, $J_{P\text{-}H} = {}^3J_{H\text{-}H}$ = 6.4 Hz, 18H, P(CH*Me*$_2$)$_3$], 2.30–2.40 [m, 6H, P(C*H*Me$_2$)$_3$], 2.57 [s, 3H, Ru=C(*Me*)OSiMe$_3$]. ^{31}P{^{1}H} NMR (162 MHz, C_6D_6, 20 °C): δ 58.6 (s). ^{13}C{^{1}H} NMR (101 MHz, C_6D_6, 20 °C): δ 1.2 [s, Ru=C(Me)OSi*Me*$_3$], 20.2 [s, P(CH*Me*$_2$)$_3$], 20.4 [s, P(CH*Me*$_2$)$_3$], 25.3 [vt, $J_{P\text{-}C}$ = 9.5 Hz, P(*C*HMe$_2$)$_3$], 43.1 [s, Ru=C(*Me*)OSiMe$_3$], 283.8 [t, $^2J_{P\text{-}C}$ = 8.4 Hz, Rû*C*(Me)OSiMe$_3$].

RuHCl(PPr$^i_3$)$_2$(=C(Me)OCH$_2$CH$_2$OBu^n). Under Ar, 20 mg (0.044 mmol) of $RuHCl(PPr^i_3)_2$ was placed in an NMR tube in C_6D_6. *Via* syringe, 7.3 μL (0.044 mmol) of ethylene glycol butyl vinyl ether was added and the tube sealed. ^{1}H, ^{13}C{^{1}H} and ^{31}P{^{1}H} NMR spectra taken after 24 h revealed quantitative conversion to $RuHCl(PPr^i_3)_2$(=C(Me)OCH$_2$CH$_2$OBu^n). ^{1}H NMR (300 MHz, C_6D_6, 20 °C): δ −21.29 (t, $^2J_{P\text{-}H}$ = 21.6 Hz, 1H, Ru*H*), 0.86 (t, $^3J_{H\text{-}H}$ = 7.5 Hz, 3H, OCH$_2$CH$_2$CH$_2$C*H*$_3$), 1.07 (apparent sextet, $^3J_{H\text{-}H}$ = 7.8 Hz, 2H, OCH$_2$CH$_2$C*H*$_2$CH$_3$), 1.17 [dvt, $J_{P\text{-}H} = {}^3J_{H\text{-}H}$ = 6.6 Hz, 18H, P(CH*Me*$_2$)$_3$], 1.30 [dvt, $J_{P\text{-}H} = {}^3J_{H\text{-}H}$ = 6.6 Hz, 18H, P(CH*Me*$_2$)$_3$], 1.49 (apparent quintet, $^3J_{H\text{-}H}$ = 7.8 Hz, 2H, OCH$_2$C*H*$_2$CH$_2$CH$_3$), 2.40–2.50 [m, 6H, P(C*H*Me$_2$)$_3$], 2.76 [s, 3H, Ru=C(*Me*)OR], 3.27 (t, $^3J_{H\text{-}H}$ = 6.9 Hz, 2H, OC*H*$_2$CH$_2$CH$_2$CH$_3$), 3.56 (t, $^3J_{H\text{-}H}$ = 4.0 Hz, 2H, OCH$_2$C*H*$_2$OBu^n), 4.56 (t, $^3J_{H\text{-}H}$ = 4.0 Hz, 2H, OC*H*$_2$CH$_2$OBu^n). ^{31}P{^{1}H} NMR (121 MHz, C_6D_6, 20 °C): δ 57.8 (s). ^{13}C{^{1}H} NMR (75.5 MHz, C_6D_6, 20 °C): δ 14.3 (s, OCH$_2$CH$_2$CH$_2$*C*H$_3$), 19.9 (s, OCH$_2$CH$_2$*C*H$_2$CH$_3$), 20.0 [s, P(CH*Me*$_2$)$_3$], 20.7 [s, P(CH*Me*$_2$)$_3$], 26.5 [vt, $J_{P\text{-}C}$ = 9.5 Hz, P(*C*HMe$_2$)$_3$], 32.4 (s, OCH$_2$*C*H$_2$CH$_2$CH$_3$), 40.8 [s, Ru=C(*Me*)OR], 69.5 (s, O*C*H$_2$CH$_2$CH$_2$CH$_3$), 71.4 (s, OCH$_2$*C*H$_2$OBu^n), 72.7 (s, O*C*H$_2$CH$_2$OBu^n), 288.7 (t, $^2J_{P\text{-}C}$ = 9.5 Hz, Ru=*C*).

RuHCl(PPr$^i_3$)$_2$(=C(Me)OCH$_2$CH$_2$OH). Under Ar, 25 mg (0.055 mmol) of $RuHCl(PPr^i_3)_2$ was placed in an NMR tube in C_6D_6. *Via* syringe, 4.9 μL (0.055 mmol) of ethylene glycol vinyl ether was added and the tube sealed. ^{1}H, ^{13}C{^{1}H}, and ^{31}P{^{1}H} NMR spectra taken after 6 h revealed conversion to $RuHCl(PPr^i_3)_2$(=C(Me)OCH$_2$CH$_2$OH). ^{1}H NMR (400 MHz, C_6D_6, 20 °C): δ −21.11 (t, $^2J_{P\text{-}H}$ = 21.6 Hz, 1H, Ru*H*), 1.13 [dvt, $J_{P\text{-}H} = {}^3J_{H\text{-}H}$ = 6.6 Hz, 18H, P(CH*Me*$_2$)$_3$], 1.26 [dvt, $J_{P\text{-}H} = {}^3J_{H\text{-}H}$ = 6.6 Hz, 18H, P(CH*Me*$_2$)$_3$], 2.36–2.46 [m, 6H, P(C*H*Me$_2$)$_3$], 2.72 [s, 3H, Ru=C(*Me*)OR], 3.53 (s, 1H, O*H*) when 10.0 mg $RuHClL_2$ and equimolar olefin are used in the same solvent volume, O*H* has δ 3.36); 3.68 (t, $^3J_{H\text{-}H}$ = 4.8 Hz, 2H, OCH$_2$C*H*$_2$OH), 4.36 (t, $^3J_{H\text{-}H}$ = 4.8 Hz, 2H, OC*H*$_2$CH$_2$OH). ^{31}P{^{1}H} NMR (162 MHz, C_6D_6, 20 °C): δ 56.4 (s). ^{13}C{^{1}H} NMR (101 MHz, C_6D_6, 20 °C): δ 19.7 [s, P(CH*Me*$_2$)$_3$], 20.4 [s, P(CH*Me*$_2$)$_3$], 26.3 [vt, $J_{P\text{-}C}$ = 10.0 Hz, P(*C*HMe$_2$)$_3$], 40.8 [s, Ru=C(*Me*)OR], 61.1 (s, OCH$_2$*C*H$_2$OH), 74.3 (s, O*C*H$_2$CH$_2$OH), 288.8 (t, $^2J_{P\text{-}C}$ = 8.4 Hz, Ru=*C*).

RuHCl(PPr$^i_3$)$_2$(=]C(Me)OCH$_2$CH$_2$OCH$_2$CH$_2$OH). Under Ar, 10 mg (0.022 mmol) of $RuHCl(PPr^i_3)_2$ was placed in an NMR tube in C_6D_6. *Via* syringe, 3.0 μL (0.022 mmol) of diethylene glycol vinyl ether was added and the tube sealed. ^{1}H and ^{31}P{^{1}H} NMR spectra taken after 1 h revealed conversion to $RuHCl(PPr^i_3)_2$(=C(Me)OCH$_2$CH$_2$OCH$_2$CH$_2$OH). ^{1}H NMR (400 MHz, C_6D_6, 20 °C): δ −21.40 (t, $^2J_{P\text{-}H}$ = 21.2 Hz, 1H, Ru*H*), 1.15 [dvt, $J_{P\text{-}H} = {}^3J_{H\text{-}H}$ = 6.8 Hz, 18H, P(CH*Me*$_2$)$_3$], 1.27 [dvt, $J_{P\text{-}H} = {}^3J_{H\text{-}H}$ = 6.8 Hz, 18H, P(CH*Me*$_2$)$_3$], 2.37–2.47 [m, 6H, P(C*H*Me$_2$)$_3$], 2.71 [s, 3H, Ru=C(*Me*)OR], δ 3.25 (t, $^3J_{H\text{-}H}$ = 4.4 Hz, 2H, OCH$_2$C*H*$_2$OH), 3.51 (m, 4H, C*H*$_2$OC*H*$_2$), 4.51 [t, $^3J_{H\text{-}H}$ = 4.4 Hz, 2H, Ru=C(*Me*)OC*H*$_2$], the OH proton is obscured by signals for the protons vicinal to the ether oxygen(s). ^{31}P{^{1}H} NMR (162 MHz, C_6D_6, 20 °C): δ 56.3 (s).

RuHCl(PPr$^i_3$)$_2$(=C(Me)OCH$_2$CH$_2$O(Me)C=)RuHCl(PPr$^i_3$)$_2$. Under Ar, 150 mg (0.328 mmol) of $RuHCl(PPr^i_3)_2$ was charged in a Schlenk flask and dissolved in 10 mL of benzene. Over a period of 1 h, 20.5 μL (0.164 mmol) of ethylene glycol divinyl ether in 5 mL of benzene was added through a pressure equalized dropping funnel and the reaction stirred overnight. The benzene was removed to a N_2 trap and the residue was dissolved in pentane. Cooling at −60 °C overnight afforded a brown precipitate that was washed with a small amount of cold pentane and dried *in vacuo*. Isolated yield: 65 mg (90% by ^{31}P{^{1}H} NMR integration before work-up). ^{1}H, ^{13}C{^{1}H}, and ^{31}P{^{1}H} NMR showed clean conversion to [$RuHCl(PPr^i_3)_2$(=C(Me)OCH$_2$–)]$_2$. ^{1}H NMR (300 MHz, C_6D_6, 20 °C): δ −21.21 (t, $^2J_{P\text{-}H}$ = 21.8 Hz, 1H, Ru*H*), 1.17 [dvt, $J_{P\text{-}H} = {}^3J_{H\text{-}H}$ = 6.4 Hz, 18H, P(CH*Me*$_2$)$_3$], 1.30 [dvt, $J_{P\text{-}H} = {}^3J_{H\text{-}H}$ = 6.4 Hz, 18H, P(CH*Me*$_2$)$_3$], δ 2.33–2.44 [m, 6H, P(C*H*Me$_2$)$_3$], 2.73 [s, 3H, Ru=C(*Me*)OCH$_2$–], 4.85 [s, 2H, Ru=C(Me)OC*H*$_2$–]. ^{31}P{^{1}H} NMR (121 MHz, C_6D_6, 20 °C):

δ 57.9 (s). $^{13}C\{^1H\}$ NMR (101 MHz, C_6D_6, 20 °C): δ 19.7 [s, $P(CHMe_2)_3$], 20.5 [s, $P(CHMe_2)_3$], 26.3 [vt, J_{P-C} = 9.7 Hz, $P(CHMe_2)_3$], 41.3 [s, Ru=C(*Me*)OCH_2–], 71.3 [s, Ru=C(Me)OCH_2–], 288.8 (t, $^2J_{P-C}$ = 9.1 Hz, Ru=*C*(Me)OCH_2–].

Preparation of 2-fluoroethyl vinyl ether: CH_2=CH(OCH_2CH_2F). Under Ar, 1.85 g (11.5 mmol) of diethylamino sulfur trifluoride (DAST)[29] was dissolved in 10 mL CH_2Cl_2. The solution was cooled to −78 °C and 1.03 mL (11.5 mmol) of ethylene glycol vinyl ether was added *via* syringe. The solution was allowed to warm to room temperature and stirred for 1 h, then cooled to 0 °C and the solvent removed to an N_2 trap. The product was then fractionally distilled, collecting the 79–81 °C fraction (760 torr). Yield : approx. 500 mg (49%). ^1H NMR (300 MHz, C_6D_6, 20 °C):δ 3.28 (dt, $^3J_{F-H}$ = 28.5 Hz, $^3J_{H-H}$ = 3.9 Hz, 2H, OCH_2CH_2F), 3.89 [dd, $^3J_{H-H}$ = 6.9 Hz, $^2J_{H-H}$ = 1.5 Hz, 1H, CH_2=CH(OR)], 4.01 [dd, $^3J_{H-H}$ = 14.1 Hz, $^2J_{H-H}$ = 1.5 Hz, 1H, CH_2=CH(OR)], 4.06 (dt, $^3J_{F-H}$ = 47.7 Hz, $^3J_{H-H}$ = 3.9 Hz, 2H, OCH_2CH_2F), 6.30 [dd, $^3J_{H-H}$ = 14.1 Hz, $^3J_{H-H}$ = 6.9 Hz, 1H, CH_2=CH(OR)]. $^{13}C\{^1H\}$ NMR (75.5 MHz, C_6D_6, 20 °C): δ 67.0 (d, $^2J_{F-C}$ = 20.5 Hz, OCH_2CH_2F), 81.5 (d, $^1J_{F-C}$ = 171 Hz, OCH_2CH_2F), 86.1 [s, CH_2=CH(OR)], 151.7 [s, CH_2=*C*H(OR)]. ^{19}F NMR (282 MHz, C_6D_6, 20 °C): δ −224.8 (tt, $^2J_{H-F}$ = 47.7 Hz, $^3J_{H-F}$ = 28.5 Hz).

RuHCl(PPr^i_3)$_2$(=C(Me)OCH_2CH_2F). Under Ar, 10 mg (0.022 mmol) of RuHCl(PPr^i_3)$_2$ was placed in an NMR tube in C_6D_6. *Via* syringe, 2.5 μL (0.022 mmol) of 2-fluoroethyl vinyl ether was added and the NMR tube sealed. ^1H, ^{19}F, and $^{31}P\{^1H\}$ NMR spectra taken after 3 h revealed quantitative conversion to RuHCl(PPr^i_3)$_2$(=C(Me)OCH_2CH_2F). ^1H NMR (300 MHz, C_6D_6, 20 °C): δ −21.32 (t, $^2J_{P-H}$ = 21.6 Hz, 1H, Ru*H*), 1.12 [dvt, J_{P-H} = $^3J_{H-H}$ = 6.3 Hz, 18H, $P(CHMe_2)_3$], 1.25 [dvt, J_{P-H} = $^3J_{H-H}$ = 6.3 Hz, 18H, $P(CHMe_2)_3$], 2.32–2.44 [m, 6H, $P(CHMe_2)_3$], 2.72 [s, 3H, Ru=C(*Me*)OR], 4.26 (dt, $^2J_{F-H}$ = 47.7 Hz, $^3J_{H-H}$ = 3.9 Hz, 2H, OCH_2CH_2F), 4.46 (dt, $^3J_{F-H}$ = 29.7 Hz, $^3J_{H-H}$ = 3.9 Hz, 2H, OCH_2CH_2F). $^{31}P\{^1H\}$ NMR (121 MHz, C_6D_6, 20 °C): δ 57.8 (s). ^{19}F NMR (282 MHz, C_6D_6, 20 °C): δ −224.1 (tt, $^2J_{H-F}$ = 47.7 Hz, $^3J_{HF}$ = 29.7 Hz).

RuHCl(PPr^i_3)$_2$(=C(Me)$OCH_2CH_2NEt_2$). Under Ar, 10 mg (0.022 mmol) of RuHCl(PPr^i_3)$_2$ was placed in an NMR tube in C_6D_6. *Via* syringe, 4.1 μL (0.022 mmol) of 2-(diethylamino) ethanol vinyl ether was added and the tube sealed. ^1H and $^{31}P\{^1H\}$ NMR spectra taken after 90 min revealed quantitative conversion to RuHCl(PPr^i_3)$_2$(=C(Me)$OCH_2CH_2NEt_2$). ^1H NMR (400 MHz, C_6D_6, 20 °C): δ −21.41 (brs, 1H, Ru*H*), 0.96 [t, $^3J_{H-H}$ = 7.2 Hz, 3H, $N(CH_2CH_3)_2$], 1.16 [dvt, J_{P-H} = $^3J_{H-H}$ = 6.4 Hz, 18H, $P(CHMe_2)_3$], 1.29 [dvt, J_{P-H} = $^3J_{H-H}$ = 6.4 Hz, 18H, $P(CHMe_2)_3$], 2.40–2.50 (m, 6H, $P(CHMe_2)_3$], 2.47 [q, $^3J_{H-H}$ = 7.2 Hz, 2H, $N(CH_2CH_3)_2$], 2.74 [s, 3H, Ru=C(*Me*)OR], 2.77 (t, $^3J_{H-H}$ = 6.8 Hz, 2H, $OCH_2CH_2NEt_2$), 4.54 (t, $^3J_{H-H}$ = 6.8 Hz, 2H, $OCH_2CH_2NEt_2$). $^{31}P\{^1H\}$ NMR (162 MHz, C_6D_6, 20 °C): δ 56.4 (s).

RuHCl(PPr^i_3)$_2$(=C(Me)OCH_2CHOCH_2). Under Ar, 10 mg (0.022 mmol) of RuHCl(PPr^i_3)$_2$ was placed in an NMR tube in C_6D_6. *Via* syringe, 2.2 μL (0.022 mmol) of glycidyl vinyl ether (racemic) was added and the NMR tube sealed. ^1H and $^{31}P\{^1H\}$ NMR spectra taken after 1 h revealed quantitative conversion to RuHCl(PPr^i_3)$_2$(=C(Me)OCH_2CHOCH_2). ^1H NMR (300 MHz, C_6D_6, 20 °C): δ −21.41 (t, $^2J_{P-H}$ = 22.2 Hz, 1H, Ru*H*), 1.15 [dvt, J_{P-H} = $^3J_{H-H}$ = 6.4 Hz, 18H, $P(CHMe_2)_3$], 1.26 [dvt, J_{P-H} = $^3J_{H-H}$ = 6.4 Hz, 18H, $P(CHMe_2)_3$], 2.22 (dd, J_{H-H} = 5.3, 2.3 Hz, 1H, OCH_2CHOCH_2), 2.30 (apparent t, J_{H-H} = 4.4 Hz, 1H, OCH_2CHOCH_2), 2.35–2.45 [m, 6H, $P(CHMe_2)_3$], 2.72 [s, 3H, Ru=C(*Me*)OR], 3.00 (m, 1H, OCH_2CHOCH_2), 4.34 (dd, J_{H-H} = 13.4, 6.3 Hz, 1H, OCH_2CHOCH_2), 4.58 (dd, J_{H-H} = 13.4, 2.1 Hz, 1H, OCH_2CHOCH_2). $^{31}P\{^1H\}$ NMR (121 MHz, C_6D_6, 20 °C): δ 56.33, 56.24 (AB pattern, $^2J_{P-P}$ = 220 Hz).

RuHCl(PPr^i_3)$_2$(=C(Me)N(Me)C(O)CH_3). Under Ar, 75 mg (0.164 mmol) of RuHCl(PPr^i_3)$_2$ was charged in a Schlenk flask and dissolved in 10 mL of benzene. *Via* syringe, 18.6 μL (0.180 mmol) of *N*-methyl-*N*-vinylacetamide was added and the solution stirred for 4 days. The benzene was removed to a N_2 trap and the purple solid was washed with pentane. Drying *in vacuo* yielded 40 mg (45%) of RuHCl(PPr^i_3)$_2$(=C(Me)N(Me)C($\dot{O}^{CH_3}$). ^1H NMR (400 MHz, CD_2Cl_2, 20 °C): δ −17.24 (t, $^2J_{P-H}$ = 26.2 Hz, 1H, Ru*H*), 0.96 [dvt, J_{P-H} = $^3J_{H-H}$ = 6.4 Hz, 18H, $P(CHMe_2)_3$], 1.28 [dvt, J_{P-H} = $^3J_{H-H}$ = 6.4 Hz, 18H, $P(CHMe_2)_3$], 2.20 [s, 3H, Ru=C(*Me*)NR_2], 2.22–2.36 [m, 6H, $P(CHMe_2)_3$], 2.43 [s, 3H, N(Me)C(O)*Me*], 3.34 [s, 3H, N(*Me*)C(O)Me]. $^{31}P\{^1H\}$ NMR (162 MHz, CD_2Cl_2, 20 °C): δ 50.4 (s). $^{13}C\{^1H\}$ NMR (101 MHz, CD_2Cl_2, −20 °C): δ 18.7 [s, $P(CHMe_2)_3$], 19.4 [s, $P(CHMe_2)_3$], 22.9 [s, N(Me)C(O)*Me*], 25.9 [vt, J_{P-C} = 8.6 Hz, $P(CHMe_2)_3$], 34.7 [s, N(*Me*)C(O)Me], 40.9 [s, Ru=C(*Me*)NR_2], 174.7 [s, N(Me)*C*(O)Me], 265.3 (t, $^2J_{P-C}$ = 9.7 Hz, Ru=*C*). ν_{CO}(CH_2Cl_2, 25 °C) = 1599 cm^{-1}.

RuHCl(PPr^i_3)$_2$(=C(Me)NC(O)$CH_2CH_2CH_2$). Under Ar, 240 mg (0.524 mmol) of RuHCl(PPr^i_3)$_2$ was charged in a Schlenk flask and dissolved in 35 mL of benzene. *Via* syringe, 60.0 μL (0.561 mmol) of 1-vinyl-2-pyrrolidinone was added and the solution stirred for 2 days. The benzene was removed to a liquid N_2 trap and the purple solid was washed with pentane. Drying *in vacuo* yielded 160 mg (90% by $^{31}P\{^1H\}$ integration before workup) of RuHCl(PPr^i_3)$_2$(=C(Me)NC(O)$CH_2CH_2CH_2$). ^1H NMR (400 MHz, CD_2Cl_2, 20 °C): δ −19.56 (t, $^2J_{P-H}$ = 25.8 Hz, 1H, Ru*H*), 0.98 [dvt, J_{P-H} = $^3J_{H-H}$ = 6.4 Hz, 18H, $P(CHMe_2)_3$], 1.27 [dvt, J_{P-H} = $^3J_{H-H}$ = 6.4 Hz, 18H, $P(CHMe_2)_3$], 2.01 [s, 3H, Ru=C(*Me*)NR_2], 2.23–2.37 [m, 6H, $P(CHMe_2)_3$], 2.32 (apparent quintet, $^3J_{H-H}$ = 7.5 Hz, 2H, $NC(O)CH_2CH_2CH_2$), 2.52 [t, $^3J_{H-H}$ = 8.0 Hz, 2H, $NC(O)CH_2CH_2CH_2$], 3.70 [t, $^3J_{H-H}$ = 7.0 Hz, 2H, $NC(O)CH_2CH_2CH_2$]. $^{31}P\{^1H\}$ NMR (162 MHz, CD_2Cl_2, 20 °C): δ 49.3 (s). $^{13}C\{^1H\}$ NMR (101 MHz, CD_2Cl_2, −20 °C): δ 19.0 [s, $P(CHMe_2)_3$], 19.6 [s, $P(CHMe_2)_3$], 22.1 [s, $NC(O)CH_2CH_2CH_2$], 25.9 [vt, J_{P-C} = 8.6 Hz, $P(CHMe_2)_3$], 29.7 [s, $NC(O)CH_2CH_2CH_2$], 40.4 [s, Ru=C(*Me*)NR_2], 45.9 [s, $NC(O)CH_2CH_2CH_2$], 180.2 [s, $NC(O)CH_2CH_2CH_2$], 261.5 (t, $^2J_{P-C}$ = 10.0 Hz, Ru=*C*). ν_{CO}(CH_2Cl_2, 25 °C) = 1640 cm^{-1}.

RuHCl(PPr^i_3)$_2$(CH_2=CH–$NC_8H_4O_2$). Under Ar, 100 mg (0.218 mmol) of RuHCl(PPr^i_3)$_2$ and 38 mg (0.218 mmol) of vinyl phthalimide were mixed and then stirred 1.5 h at room temperature. The solvent was removed and the product dried *in vacuo*. Yield: quantitative. ^1H NMR (400 MHz, THF-d_8, 0 °C): δ −20.83 (dd, $^2J_{P-H}$ = 15.6, 27.6 Hz, 1H, Ru*H*), 1.10 [dvt, J_{P-H} = $^3J_{H-H}$ = 7.6 Hz, 9H, $P(CHMe_2)_3$], 1.25 [m, 29H, $P(CHMe_2)_3$], 1.64 (brd, 1H, J_{H-H} = 3.2 Hz, CH_2=CH–$NC_8H_4O_2$), 2.41 (dd, 1H, J_{H-H} = 14.0, 4.4 Hz, CH_2=CH–$NC_8H_4O_2$), 2.74 [br s, 3H, $P(CHMe_2)_3$], 2.85 [brs, 3H, $P(CHMe_2)_3$], 4.74 (ddd – apparent dt, 1H, J_{H-H} = 14.6, 6.4 Hz, CH_2=CH–$NC_8H_4O_2$), 7.82 (m, 4H, CH_2=CH–$NC_8H_4O_2$). $^{31}P\{^1H\}$ NMR (162 MHz, THF-d_8, 0 °C): δ 35.4, 57.9 (AX pattern, J_{P-P} = 278 Hz). $^{13}C\{^1H\}$ NMR (101 MHz, THF-d_8, −20 °C): δ 19.5, 19.8, 20.16, 20.22 [s, $P(CHMe_2)_3$], 24.1 [d, J_{P-C} = 11.1 Hz, $P(CHMe_2)_3$], 24.8 [d, J_{P-C} = 16.1 Hz, $P(CHMe_2)_3$], 29.8 (s, CH_2=CH–$NC_8H_4O_2$), 60.2 (s, CH_2=CH–$NC_8H_4O_2$), 124.1, 124.7, 129.1, 130.8, 135.4 (s, CH_2=CH–$NC_8H_4O_2$ aromatics; the peak at 135.4 is over twice as large as the others and arises from two signals with coincidental overlap), 167.0, 176.6 (s, CH_2=CH–$NC_8H_4O_2$ carbonyls).

$RuHCl(PPr^i_3)_2$ with 9-vinyl carbazole. Under Ar, 10 mg (0.022 mmol) of $RuHCl(PPr^i_3)_2$ and 4.3 mg (0.022 mmol) of 9-vinyl carbazole were placed in an NMR tube in C_6D_6 at 25 °C. ^1H, and $^{31}P\{^1H\}$ NMR spectra taken after 1 h revealed approximately 30% conversion to an olefin adduct. In addition, broadened signals for $RuHClL_2$ and the free olefin are observed. In addition, an argument for bonding though the olefinic portion of the reactant is strengthened by the RuH signal being more complicated than a triplet. Adduct: ^1H NMR (300 MHz, C_6D_6, 20 °C): δ −19.52 (m, Ru*H*), olefinic protons appear to be buried under signals from the PPr^i_3 ligands. $^{31}P\{^1H\}$ NMR (121 MHz, C_6D_6, 20 °C): δ 38.6, 47.3 (AB pattern, $^2J_{P\text{-}P} = 290$ Hz).

$RuHCl(PPr^i_3)_2$ with 3-methylene-2,3-dihydrofuran. Treatment of 3-furaldehyde with hydrazine in ethylene glycol[30] leads to a mixture of 62% 3-methylene-2,3-dihydrofuran and 38% 3-methylfuran.

Addition of 10 equiv. of the conjugated diene to a solution of 10 mg $RuHCl(PPr^i_3)_2$ in 0.5 mL of C_6D_6 results in complete isomerization to 3-methylfuran within 10 min. No reaction occurs from the 3-methylfuran with $RuHCl(PPr^i_3)_2$ at room temperature over several hours.

Preparation of CH_2=CD(OEt). The isotopically labeled olefin was prepared by hydrolysis of CH_2=C(Li)OEt[31] with an excess of D_2O in *o*-xylene at −10 °C. Filtration and fractional distillation (30–35 °C fraction) of the resulting mixture yielded 99% enriched CH_2=C(D)OEt by ^1H NMR.

Preparation of $RuDCl(PPr^i_3)_2$. Method 1: $RuD_2Cl_2(PPr^i_3)_2$ was prepared with 99% enrichment by stirring $RuH_2Cl_2(PPr^i_3)_2$ under an atmosphere of D_2 in CH_2Cl_2 for 4 h at 25 °C. The head space gases were removed and the flask refilled with D_2 once during this time period. The crude $RuD_2Cl_2(PPr^i_3)_2$ was then washed with ether and dried *in vacuo*, then dehydrohalogenated.

Method 2 : $RuDCl(PPr^i_3)_2$ was prepared by stirring $RuHCl(PPr^i_3)_2$ in a small amount of acetone-d_6 for 12 h at 25 °C to allow isotopic exchange through the enol tautomer of the acetone-d_6. Solution NMR shows >90% of the D incorporation now located in the PPr^i_3 methyl groups. This is consistent with agostic stabilization of $RuHClL_2$ by the PPr^i_3 ligand(s).

X-Ray structure determinations

$RuHCl(PPr^i_3)_2(C_6H_9NO)$. Data were corrected for absorption and Lorentz and polarization effects and equivalent reflections were then averaged. The structure was solved using direct methods (MULTAN78) and Fourier techniques. Two methylene carbons of the C_5 ring show 50 : 50 disorder, which was easily modeled. Hydrogen atoms were placed in fixed, idealized positions for the carbon atoms of the ligands, and a difference Fourier examined to locate the metal hydride. All hydrogen atoms were refined isotropically except those associated with the disordered carbon atoms. A final difference Fourier was featureless, with the exception of several peaks of density 1.3–3.02 e $Å^{-3}$ lying at the metal site. These are undoubtedly due to inaccuracies in the absorption correction.

$RuHCl(N_2)(PPr^i_3)_2$. Data were collected by the moving crystal-moving detector technique with fixed background counts at each extreme of the scan. Data were corrected for Lorentz and polarization effects, and equivalent data were averaged. The structure was solved by direct methods (SHELXTL) and Fourier techniques. All carbon-bound hydrogen atoms were located in a difference electron density map phased on the nonhydrogen atoms, and were included as isotropic contributors in the final cycles of least-squares refinement. The thermal parameter of hydrogen atom H(10) was fixed in the final cycles of least-squares to prevent it from refining to a negative value; no other restraints or constraints were applied. No attempt was made to locate the presumed hydride ligand. The molecule contains one Cl^- and one N_2 ligand, disordered with each other through the center of symmetry at the site of the ruthenium atom. Although the occupancies of these disordered ligands were fixed in the final refinement, prior refinements in which those occupancies were permitted to vary yielded the same occupancies within 1.5 standard uncertainties. However, the structural parameters of the N_2 ligand are not accurately determined due to this systematic error. A final difference Fourier map was featureless, with the largest peak having an intensity of only 0.38 e $Å^{-3}$ and residing near the ruthenium atom.

CCDC reference number 440/154. See http://www.rsc.org/suppdata/nj/a9/a907624G/ for crystallographic files in .cif format.

Acknowledgements

This work was supported by the U.S. NSF, the Université de Montpellier and the French CNRS.

References

1 J. N. Coalter, G. J. Spivak, H. Gérard, E. Clot, E. R. Davidson, O. Eisenstein and K. G. Caulton, *J. Am. Chem. Soc.*, 1998, **120**, 9388.
2 D. Huang, G. J. Spivak and K. G. Caulton, *New J. Chem.*, 1998, **22**, 1023.
3 J. N. Coalter, J. C. Huffman, W. E. Streib and K. G. Caulton, manuscript in preparation.
4 We propose that the ^1H chemical shift for R = Cy, $SiMe_3$, and $CH_2CH_2CH_2$ (cyclic) are slightly downfield from that of R = Et as a result of the influence on the hydride of changing angle Cl–Ru=C due to electronic and steric factors with the bulkier R groups.
5 Remarkably, 2,3-dihydropyran, the six-membered ring analog, fails to react after 12 h at 25 °C.
6 (*a*) P. Schwab, R. H. Grubbs and J. W. Ziller, *J. Am. Chem. Soc.*, 1996, **118**, 100; (*b*) S. T. Nguyen, L. K. Johnson, R. H. Grubbs and J. W. Ziller, *J. Am. Chem. Soc.*, 1992, **114**, 3974; (*c*) Z. Wu, S. T. Nguyen, R. H. Grubbs and J. W. Ziller, *J. Am. Chem. Soc.*, 1995, **117**, 5503; (*d*) P. Schwab, M. B. France, J. W. Ziller and R. H. Grubbs, *Angew. Chem., Int. Ed. Engl.*, 1995, **34**, 2039.
7 Slower reaction rate with H_2C=CD(OEt) permits observation of this AB NMR pattern even at 25 °C.
8 Even if H_2C=CD(OEt) is reacted with $RuHClL_2$ (2 : 1 mole ratio) at 25 °C to minimize the time spent as the olefin adduct, D is found statistically in RuD, $Ru=CC(H,D)_3(OEt)$ and all three vinylic positions of free ethyl vinyl ether; this procedure only serves to decrease the deuteration in the phosphine methyl groups.
9 A. G. Orpen, L. Brammer, F. H. Allen, O. Kennard, D. G. Watson and R. Taylor, *J. Chem. Soc., Dalton Trans.*, 1989, S1.
10 F. Ford, T. Yuzawa, M. S. Platz, S. Matzinger and M. Fülscher, *J. Am. Chem. Soc.*, 1998, **120**, 4430.
11 T. J. Johnson, A. Albinati, T. F. Koetzle, O. Eisenstein, J. C. Huffman and K. G. Caulton, *Inorg. Chem.*, 1994, **33**, 4966.
12 M. Oliván, E. Clot, O. Eisenstein and K. G. Caulton, *Organometallics*, 1998, **17**, 3091.
13 M. M. Gallo, T. P. Hamilton and H. F. Schaefer, *J. Am. Chem. Soc.*, 1990, **112**, 8714.
14 J. Silvestre and R. Hoffmann, *Helv. Chim. Acta*, 1985, **68**, 1461. Y. Wakatsuki, N. Koga, H. Werner and K. Morokuma, *J. Am. Chem. Soc.*, 1997, **119**, 360.
15 S. F. Vyboishchikov and G. Frenking, *Chem. Eur. J.*, 1998, **4**, 1428.
16 A. F. Hill, W. R. Roper, J. M. Waters and A. H. Wright, *J. Am. Chem. Soc.*, 1983, **105**, 5939.
17 C. P. Casey, C. J. Czerwinski, D. P. Powell and R. K. Hayashi, *J. Am. Chem. Soc.*, 1997, **119**, 5750.

18 (*a*) A. Cutler, S. Raghu and M. Rosenblum, *J. Organomet. Chem.*, 1974, **77**, 371; (*b*) T. C. T. Chang, M. Rosenblum and S. B. Samuels, *J. Am. Chem. Soc.*, 1980, **102**, 5931; (*c*) H. Chen and W. D. Harman, *J. Am. Chem. Soc.*, 1996, **118**, 5672.
19 W. D. Harman, *Chem. Rev.*, 1997, **97**, 1953.
20 J. S. Freundlich, R. R. Schrock and W. M. Davis, *J. Am. Chem. Soc.*, 1996, **118**, 3643.
21 M. J. Frisch, G. W. Trucks, H. B. Schlegel, P. M. W. Gill, B. G. Johnson, M. A. Robb, J. R. Cheeseman, T. Keith, G. A. Petersson, J. A. Montgomery, K. Raghavachari, M. A. Al-Laham, V. G. Zakrzewski, J. V. Ortiz, J. B. Foresman, C. Y. Peng, P. Y. Ayala, W. Chen, M. W. Wong, J. L. Andres, E. S. Replogle, R. Gomperts, R. L. Martin, D. J. Fox, J. S. Binkley, D. J. Defrees, J. Baker, J. P. Stewart, M. Head–Gordon, C. Gonzalez and J. A. Pople, *GAUSSIAN 94*, *Revision B3*, Gaussian Inc., Pittsburgh, 1995.
22 A. D. Becke, *J. Chem. Phys.*, 1993, **98**, 5648.
23 P. G. Hay and W. R. Wadt, *J. Chem. Phys.*, 1985, **82**, 299.
24 W. R. Wadt and P. J. Hay, *J. Chem. Phys.*, 1985, **82**, 284.
25 A. H. Höllwarth, M. B. Böhme, S. Dapprich, A. W. Ehlers, A. Gobbi, V. Jonas, K. F. Köhler, R. Stegmann, A. Veldkamp and G. Frenking, *Chem. Phys. Lett.*, 1993, **208**, 237.
26 P. C. Hariharan and J. A. Pople, *Theor. Chem. Acta*, 1973, **28**, 213.
27 C. Grünwald, O. Gevert, J. Wolf, P. González-Herrero and H. Werner, *Organometallics*, 1996, **15**, 1960.
28 T. E. Wilhelm, T. R. Belderrain, S. N. Brown and R. H. Grubbs, *Organometallics*, 1997, **16**, 3867.
29 W. J. Middleton, *J. Org. Chem.*, 1975, **40**, 574.
30 W. Miles, C. Berreth and P. Smiley, *Tetrahedron Lett.*, 1993, **34**, 5221.
31 R. Knorr and T. Roman, *Angew. Chem., Int. Ed. Engl.*, 1984, **23**, 366.

Paper a907624g